ISHRAE - STUDENT RESEARCH PROJECT GRANT

FINAL PROJECT REPORT

"DEVELOPMENT OF SMART REGENERATIVE EVAPORATIVE COOLER FOR STAFF CABIN ROOM"

Submitted by

19F009 - BORRIS LEO S

19F028 - NAVIN KUMAR G

19F064 - JEYA SHANKAR P

IV yr., Thiagarajar College of Engineering, Madurai

NAME OF THE GUIDE

Dr. G. KUMARAGURUPARAN

Professor,

Department of Mechatronics,

Thiagarajar College of Engineering,

Madurai - 15.

NAME OF THE MENTOR

N. BALACHANDRAN

Proprietor,

Shree Engineering,

Madurai.

BONAFIDE CERTIFICATE

This is to certify that this Project Report entitled **"DEVELOPMENT OF SMART REGENERATIVE EVAPORATIVE COOLER FOR STAFF CABIN ROOM",** submitted to ISHRAE-Student Research Project Grant, Delhi, is a bonafide record of work done by **Mr. Borris Leo S (19F009), Mr. Navin Kumar G (19F028)** and **Mr. Jeya Shankar P (19F064)** Final year students, Department of Mechatronics, Thiagarajar college of engineering under my supervision.

Signature of the Guide
Dr.G.Kumaraguruparan
Professor
Thiagarajar College of Engineering

DECLARATION BY AUTHOR(S)

This is to declare that this report has been written by us. No part of the report is plagiarized from other sources. All information included from other sources have been duly acknowledged. We aver that if any part of the report is found to be plagiarized, we shall take full responsibility for it.

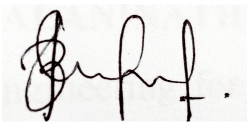

Mr. Borris Leo S
(STUDENT)

Mr. Navin Kumar G
(STUDENT)

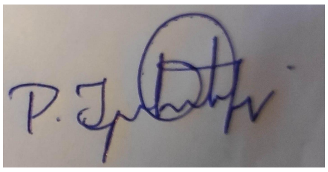

Mr. Jeya Shankar P
(STUDENT)

LIST OF CONTENTS

LIST OF SYMBOLS/ ABBREVIATIONS

Symbol / Abbreviation	Description
GWP	Global Warming Potential
DEC	Direct Evaporative Cooler
IEC	Indirect Evaporative Cooler
REC	Regenerative Evaporative Cooler
HRV	Heat Recovery Ventilator
HMX	Heat and Mass Exchanger
MIEC	Mini Indirect Evaporative Cooler
COP	Coefficient of Performance
MAE	Mean Absolute Error
RMSE	Root Mean Square Error

MVC	Mechanical Vapor Compression
SVR	Support Vector Regression
PUE	Power Usage Effectiveness
EER	Energy Efficiency Ration
NTU	Number of Transfer Units
OMBC	Open Maisotsenko-Brayton cycle
ORBC	Open Regenerative Brayton cycle
DPEC	Dew-Point Evaporative Cooler
GNN	GMDH-type Neural Network
CFD	Computational Fluid Dynamics
IR	Infrared
TDMA	Tri Diagonal Matrix Algorithm
CAD	Computer Aided Design
PWM	Pulse Width Modulation

DBT	Dry Bulb Temperature
WBT	Wet Bulb Temperature
DP	Dew Point
RH	Relative Humidity
m	metre
hr	hour
s	second
W	Watt
A	Ampere
V	Voltage
Pa	Pascal
°C	Celcius
MW	Mega Watt
ρ	density

u	velocity component in x-direction
v	velocity component in y-direction
w	velocity component in z-direction
t	time
g	gravitational acceleration
μ	viscosity
S_{ω}	rotating flow
S_{DR}	distributed resistance
k	thermal conductivity
q_V	volumetric heat source
C_p	constant pressure specific heat
r	distance from the rotation axis

LIST OF FIGURES

LIST OF TABLES

ABSTRACT

This project focuses on the design and development of regenerative cycle based indirect evaporative coolers. The usage of conventional vapor compression cycle based air-conditioning creates an impact on climate change. Additionally, the increase of Global Warming Potential (GWP) and deficiency of energy resources are also caused. This demands an alternative cooling technology such as evaporative cooling for achieving sustainable solutions for thermal comfort. The regenerative type of evaporative cooling which is better in cooling aspects than the other types is employed for the design. The wet channel of the system which acts as the heat and mass exchanger (HMX) is analyzed for uniform flow distribution for higher cooling effectiveness. The analysis of the geometry is done using Computational Fluid Dynamics (CFD) in which the outlet velocity of the fluid at each tube ranges form 0.515 to 0.521 m/s at inlet velocity of 3.88 m/s. The simulation result shows that the fluid through the wet channel is evenly distributed at all tubes. The experimental setup is fabricated using the developed design and the output parameters of the setup based on the inlet conditions are observed. The experimental results show that the temperature difference between the system's inlet and the outlet of 2.5 ℃ is achieved with relatively lesser change in humidity in the range of approximately 4%.

CHAPTER 1
INTRODUCTION

1.1 INTRODUCTION

Air-conditioning is a technology that has become an essential part of modern life. Climate change has led to more frequent and intense heat waves, making it difficult to maintain a comfortable indoor environment. From maintaining comfortable indoor temperatures to improving air quality, the benefits of air conditioning are numerous. This has shifted air conditioning from being considered a luxury to a necessity especially in arid and semi-arid climatic conditions.

Despite its advantages, air conditioning contributes to climate change. Utilizing air conditioning increases energy consumption and greenhouse gas emissions, both of which contribute to raising the Global Warming Potential (GWP). It is crucial to adopt energy-efficient models and look into alternate cooling techniques in order to reduce the detrimental effects of air conditioning on climate change.

One of the potential alternative technologies is evaporative cooling, which is much more energy-efficient than traditional air conditioning systems. Evaporative coolers can reduce energy consumption by up to 90% compared to air conditioning units. Evaporative cooling systems also have a lower carbon footprint than air conditioning units as they do not use refrigerants that contribute to greenhouse gas emissions. These systems use water as the cooling medium, which is a much more sustainable option.

This means evaporative coolers are not only cost-effective but also have a significantly lower environmental impact such as less energy consumption , non-refrigerant working and low GWP.

1.2 EVAPORATIVE COOLING

Evaporative cooling systems work on the principle of evaporation, that leads to an exchange of heat and mass during the cooling process. This eco-friendly technology uses natural refrigerant which is water (R-718) as the cooling medium.

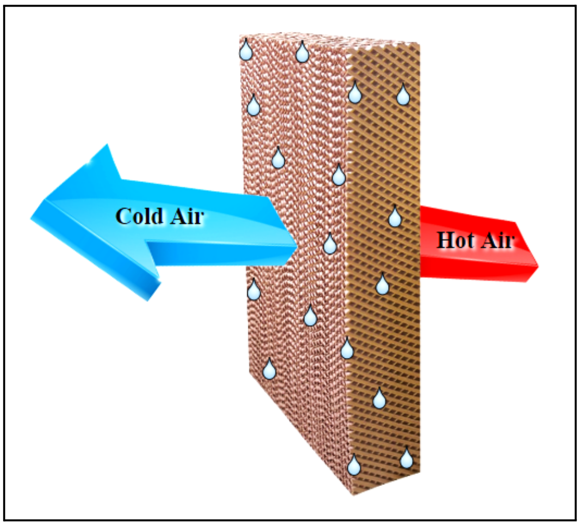

Fig.1.1. Evaporative cooling

One of the key components of an evaporative cooling system is the cooling pads which are designed to enhance the surface area of the water in contact with the air, allowing for maximum evaporation and cooling. These pads are typically made from a material such as cellulose or synthetic fibers, which can hold a lot of water without getting overly saturated.

When hot air is drawn through the evaporative cooling system, it passes over the pads that evaporate the water in the pad to cool the air. The cooled air is distributed through a blower providing relief from hot and dry weather conditions which in turn can effectively and efficiently operate to provide thermal comfort.

1.3. TYPES OF EVAPORATIVE COOLING

Basically, evaporative cooling systems can be classified into three categories. The types are as follows are:

1. **Direct Evaporative Cooler (DEC)**
2. **Indirect Evaporative Cooler (IEC)**
3. **Regenerative Evaporative Cooler (REC)**

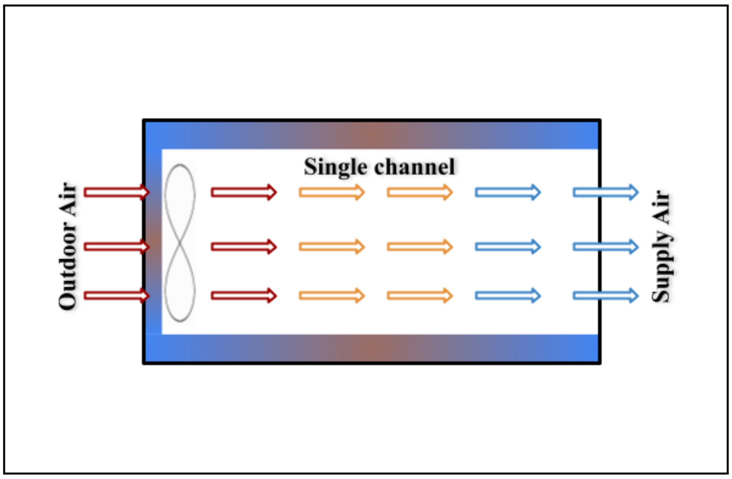

Fig. 1.2. Working of DEC

Direct evaporative coolers are the most prevalent kind of evaporative cooling systems, and are also known as single-stage coolers. In order for these systems to function, hot and dry air from the outside passes through wet pads or media. As the air flows over the moist surface, it evaporates the water, which cools the air and increases its humidity. The cooled and humidified air is directly distributed throughout the space. These coolers are a popular option for household and small business applications since they are very easy to install and operate at low cost.

They are most effective in hot, dry climates where the air is relatively dry and the humidity is low. However, they are less effective in areas with high humidity, as the cooling effect is reduced in the presence of moisture.

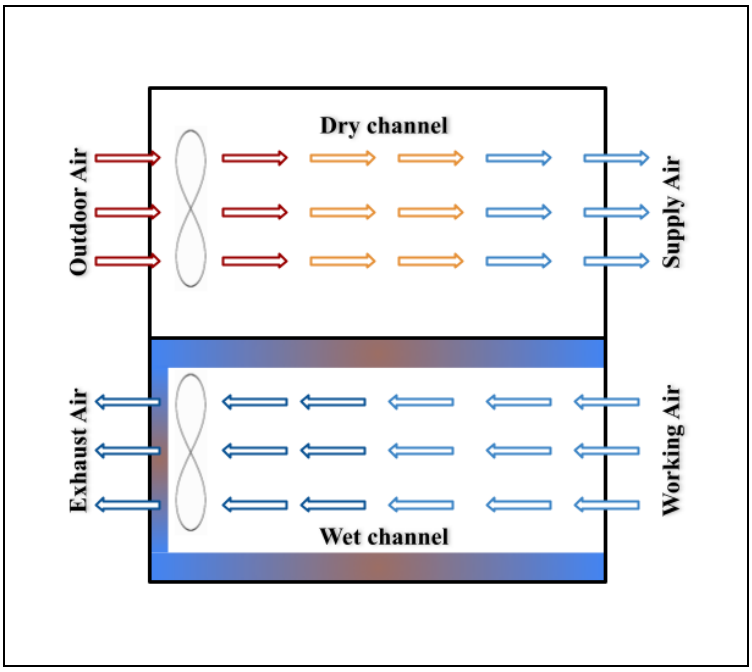

Fig. 1.3. Working of IEC

Indirect evaporative coolers, also known as two-stage evaporative coolers, use a heat exchanger to cool the air. Unlike direct evaporative coolers, the process involves two separate airstreams: the supply airstream and the working airstream. The supply airstream is cooled indirectly by passing it over a heat exchanger that is cooled by the working airstream. The working airstream is cooled directly by the evaporative cooling process, typically using a water-soaked pad. This cooled air is then passed over the heat exchanger to indirectly cool the supply airstream. Hence, the supply air indirectly cooled by the working airstream is distributed throughout the space. The primary advantage of indirect evaporative coolers is that they do not add moisture to the process air stream, making them suitable for use in humid environments where adding additional moisture would be detrimental.

They have the potential for higher cooling efficiency than direct evaporative coolers in high humidity regions, as they can achieve lower temperatures without adding moisture to the air. However, indirect evaporative coolers tend to be more complex and inefficient than direct evaporative coolers due to the need for a heat exchanger and additional components.

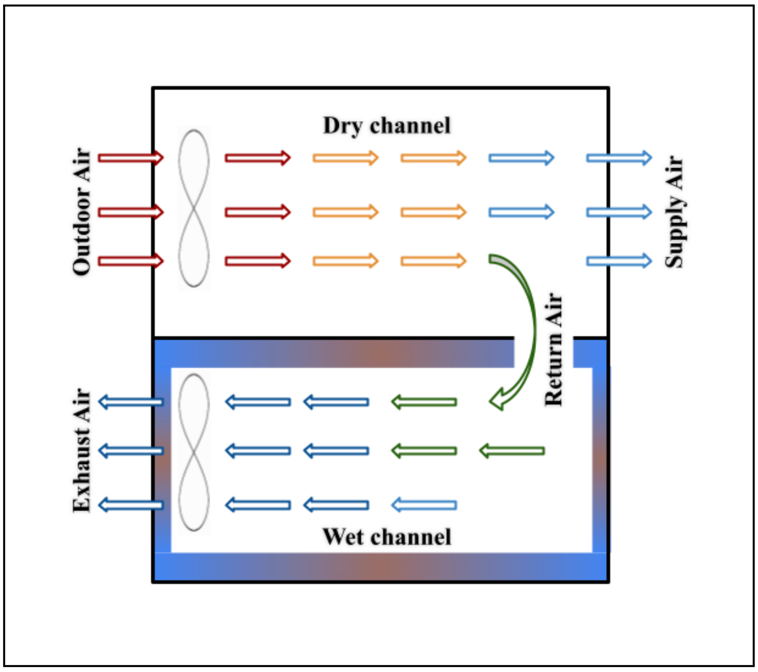

Fig. 1.4. Working of REC

Regenerative evaporative coolers, also known as Maisotsenko cycle (M-cycle) evaporative coolers work by using a heat exchanger to pre-cool incoming air before it passes through a cooling pad. The heat exchanger consists of two channels: one that carries incoming hot and dry air and another that carries cool and moist air from the split from the first channel. As the incoming hot and dry air passes through the one channel of the heat exchanger, some amount of air is regenerated to another channel.This pre-cooling process reduces the temperature and humidity of the incoming air, making it easier to cool further in the cooling pad. The cooled air then passes through the cooling pad, where it is further cooled as it passes through the wet pad material. The temperature of the supply air reduces eventually as the working air gets saturated, which is continuously distributed throughout the space through fans or blowers.

This means that the regenerative evaporative cooling is a highly efficient and effective cooling method for both humid and less humid regions, capable of delivering cool and comfortable air with minimal energy consumption and environmental impact than DEC and IEC methods.

Evaporative cooling system type	Positive aspects	Possible drawback
DEC	Energy efficient due to its simple structure and high cooling efficiency	High humid air outlet
IEC	Less humid supply air than DEC, possibly can provide dry air	Less cooling efficiency than DEC
REC	Less humid air with higher cooling efficiency than IEC	Expensive and complex in construction than the previous types

Table 1.1. Types of evaporative cooling system and their scope

1.3. ORGANIZATION OF THE REPORT

The report includes the following 7 chapters:

- Chapter 1 discusses the challenges of using conventional air-conditioners, need of evaporative coolers and includes types and their scopes.
- Chapter 2 explains a detailed literature review of previous studies.
- Chapter 3 emphasis on the research gaps identified via literature review.
- Chapter 4 focuses on the objectives of the work and the methodology to be followed to complete the work.
- Chapter 5 explains the design of the wet channel geometry and numerical analysis of the geometry for uniform flow distribution.
- Chapter 6 illustrates the design development of the complete system with its dimensions and other features.
- Chapter 7 focuses on the fabrication of the system which includes the system fabrication as well as circuit development.

CHAPTER 2
LITERATURE REVIEW

S. Chakraborty et al. [1] presents an experimental and modeling study of an M-cycle indirect evaporative cooler (IEC) integrated with a Heat Recovery Ventilator (HRV) for use in commercial buildings.The experiments on Heat and Mass Exchanger (HMX) core of a cross-flow IEC/HRV prototype consisting of five cores with maximum flow rate of 442 m^3/hr, made of polyethylene infused with biocide were performed under different ambient conditions and ventilation rates. The results show that the M-cycle IEC achieved a cooling effectiveness of up to 94% and a sensible heat ratio of around 0.8, indicating a high level of cooling and moisture removal. The HRV achieved an efficiency of up to 85% in recovering heat from the exhaust air stream, which can be used to preheat the incoming fresh air. The mathematical model developed in the study showed good agreement with the experimental data, with an average absolute error of less than 5% for the predicted cooling effectiveness and sensible heat ratio.

C. Zhan et al. [2] investigated a cross-flow heat exchanger for indirect evaporative cooling using the M-cycle process by optimizing the design of the heat exchanger for maximum heat transfer efficiency and cooling performance. The simulations revealed that increasing the air flow rate or decreasing the water flow rate improved the effectiveness of the heat exchanger and also showed that increasing the number of channels or decreasing the channel width improved the effectiveness of the heat exchanger. However, increasing the water flow rate beyond a certain point did not result in any significant improvement in effectiveness. The comparison results show that the designed M-cycle heat and mass exchanger is able to achieve 16.7% higher cooling effectiveness compared with the conventional cross-flow heat and mass exchanger for the indirect evaporative cooler with the cooling capacity of 456.2 W.

H.S. Dizaji et al. [3] proposed and conceptualized the Mini Indirect Evaporative Cooler (MIEC) and its applicability as a local cooling process of electronic units. The study proposed a compact design for the cooler, which utilized the Maisotsenko cycle to achieve high cooling efficiency which included a 3D printed experimental setup prototype cooler with a cross-flow heat exchanger and a wet channel made of aluminum fins. The setup showed a maximum temperature drop occurred at an inlet mass flow rate of 0.008 achieving a cooling capacity of up to 93 W with an energy consumption of 1.8 W and a Coefficient of Performance (COP) of 51.7. This study provided a promising concept for a compact and efficient cooler using the Maisotsenko cycle. However, further research and development are needed to optimize the design and evaluate the practical feasibility of the proposed cooler for electronic cooling applications.

A.K. Gupta et al. [4] conducted experiments on a regenerative evaporative cooler with varying operating conditions such as inlet air temperature, relative humidity, and flow rate to generate a dataset and then used the dataset to train a machine learning model using the support vector regression algorithm. The model was evaluated based on performance metrics such as coefficient of determination (R^2), Mean Absolute Error (MAE), and Root Mean Square Error (RMSE). The model achieved an R^2 value of 0.994, indicating a strong correlation between predicted and actual performance. The MAE and RMSE values were found to be 0.017 and 0.032, respectively, indicating that the model is accurate in predicting the performance of the regenerative evaporative cooler. The high accuracy achieved by the model suggested that it can be used to optimize the operation of the cooler and improve its energy efficiency.

U. Sajjad et al.'s [5] review of recent developments in indirect evaporative cooling (IEC) technology included a thorough discussion of design factors for IEC systems, such as the material selection for the heat exchanger and wet surface, airflow rate, and water supply rate. Other cooling technologies, such as air conditioning, mechanical refrigeration, and direct evaporative cooling, were compared to the efficiency of IEC systems. According to the study, depending on the airflow velocity and heat exchanger configuration, the pressure drop across the heat exchanger ranges from 5 Pa to 150 Pa, and the cooling effectiveness of a cross-flow IEC system can range from 60% to 90% depending on the design and operating conditions. The study also demonstrated that IEC systems provide a number of benefits over alternative cooling methods, including superior cooling performance, little energy use, and minimal environmental impact.

S. Kumar et al. [6] compares the performance of two types of evaporative cooling pads, static and dynamic, under different climatic conditions and conducted experiments in an experimental setup simulating various climatic conditions, including hot and dry, hot and humid, and temperate. The wet bulb temperature, dry bulb temperature, and relative humidity at the inlet and outlet of the cooling pads were measured and the effectiveness of each pad was calculated. The results show that the dynamic pad had a cooling effectiveness ranging from 70% to 93%, while the static pad had a cooling effectiveness ranging from 55% to 87%. The pressure drop across the dynamic pad ranged from 10.6 Pa to 24.3 Pa, while the pressure drop across the static pad ranged from 12.4 Pa to 35.6 Pa. The results also show that the dynamic pad outperformed the static pad in all climatic conditions tested. The dynamic pad was found to have a higher cooling effectiveness and a lower pressure drop across the pad.

S. D. Kadam et al. [7] presented a study on the implementation of passive evaporative cooling measures in the campus of the Indian Institute of Technology (IIT) Gandhinagar and discussed the importance of reducing energy consumption in buildings and introduced passive cooling techniques as an effective way to achieve this goal, which included the use of porous ceramic evaporative cooling pads and a water fountain in a central courtyard, as well as the use of shading devices and thermal insulation. The temperature and relative humidity measurements in the campus during the summer season and compared them with data from the previous year, when the cooling measures were not in place. The results showed a significant reduction in indoor and outdoor temperatures and an increase in relative humidity, indicating improved thermal comfort conditions and estimated a reduction of about 40% in the annual cooling energy consumption.

Q. Chen et al. [8] presented an experimental investigation of a sustainable cooling process that combines indirect evaporative cooling (IEC) and Mechanical Vapor Compression (MVC) systems with the experimental setup consisting of an IEC unit and an MVC unit connected in parallel. The performance of the combined system is evaluated under different operating conditions. The conducted experiment showed that the combined system achieves a higher cooling capacity and a lower energy consumption compared to the standalone MVC system. The cooling capacity of the combined system is found to increase with an increase in the inlet air temperature of the IEC unit. At an inlet air temperature of 40 °C, the cooling capacity of the combined system is about 2.5 times that of the standalone MVC system. The result also shows that the energy consumption of the combined system is found to decrease with an increase in the inlet air temperature of the IEC unit. At an inlet air temperature of 40 °C, the energy consumption of the combined system is about 44% lower than that of the standalone MVC system.

H. M. Afsahan et al. [9] developed an artificial intelligence-based approach for predicting the thermal performance of evaporative cooling systems by using data from an experimental setup consisting of an indirect evaporative cooler and a cooling tower to train and test the machine learning models. The results show that the Support Vector Regression (SVR) algorithm provided the best predictive performance compared to other machine learning algorithms. The SVR model achieved a Mean Absolute Error (MAE) of 0.607 for predicting the wet bulb temperature and 0.489 for predicting the dry bulb temperature. This study also compared the performance of the machine learning models with a mathematical model and found that the SVR model outperformed the mathematical model and also demonstrated the potential of using artificial intelligence for predicting the thermal performance of evaporative cooling systems and highlighted the superiority of the SVR algorithm for this application.

D. Pandelidis et al. [10] investigated the performance of a cross-flow Maisotsenko cycle (M-cycle) in a humid climate with the aim of evaluating its effectiveness in improving the efficiency of evaporative cooling and presented a detailed numerical simulation of the M-cycle, followed by an experimental investigation to validate the simulation results. The effect of various design parameters on the performance of the M-cycle, such as the height and thickness of the plates, and the air flow rate were investigated and concluded that the optimum design parameters depend on the specific application, but suggest that a plate height of 10mm and a flow rate of 1.5m/s can provide good performance in humid conditions. The paper presented a detailed study of the performance of the cross-flow M-cycle in humid conditions, and provides valuable insights into the design and optimization of M-cycle systems for evaporative cooling applications. The simulation and experimental results presented in the paper are supported by numerical and statistical analysis.

J. Chu et al. [11] detailed the technical principles, evaluation indicators, system forms, and research progress of the Data Center's air-side, water-side and freon-side evaporative cold coagulation heat air conditioning systems. To lower the energy consumption of the Data Center's refrigeration and air-conditioning system, the application settings and scenarios of the various types of evaporative cooling air-conditioning systems should be thoroughly evaluated. The experimental comparisons were done and concluded that evaporative cooling air-conditioning systems can reduce the data center's yearly Power Usage Effectiveness (PUE) to less than 1.25, which has a high promotional value in data center applications. The application conditions and scenarios for the various types of evaporative cooling air-conditioning systems in data centers should be thoroughly considered in order to maximize the use of renewable energy-dry air energy in data center air-conditioning systems, thereby reducing data center air-conditioning system energy consumption.

S. Kashyap et al. [12] proposed a novel dual-mode evaporative cooler that can operate in two modes: Direct Evaporative Cooling (DEC) mode and Indirect Evaporative Cooling (IEC) mode, with indirect cooling in IEC mode combined with direct evaporative cooling in DEC mode. Experiments were conducted from May to September, and the findings demonstrate that the suggested dual-mode evaporative cooler outperforms the traditional air conditioning system in terms of Energy Efficiency Ratio (EER), cooling capacity, and power usage. The dual-mode evaporative cooler achieved an average EER of 20.54 in IEC mode and 13.33 in DEC mode, while the conventional air conditioning system achieved an average EER of 3.75. The cooling capacity of the dual-mode evaporative cooler was higher than that of the conventional air conditioning system in all months except for May. Additionally, the power consumption of the dual-mode evaporative cooler was significantly lower than that of the conventional air conditioning system in all months.

R. Boukhanouf et al. [13] presented a detailed description of the design of the REC, which incorporates a recirculating water system that cools the air and removes humidity through evaporation. The REC's performance is assessed using a mathematical model based on the conservation of mass and energy equations, and the REC's performance is measured in terms of cooling capacity, efficacy, and energy efficiency. According to the study's findings, the REC has a cooling capacity of up to 12 kW and an effectiveness of up to 80% for the conditions evaluated. The REC's energy efficiency is shown to be better than that of a traditional direct evaporative cooler, making it a viable technology for cooling buildings in arid conditions. This study gave insights into the design and performance of a regenerative evaporative cooler and indicates its potential for application in cooling buildings in arid conditions.

A. K. Dhamneya et al. [14] presented a thermodynamic performance analysis of a direct evaporative cooling system with increased heat and mass transfer area. The aim of the study is to improve the cooling efficiency of the system by increasing the heat and mass transfer area. The analysis is based on a mathematical model that considers the energy and mass balance equations for the cooling pad, air duct, and fan. The effectiveness-NTU (Number of Transfer Units) method is used to evaluate the heat transfer in the cooling pad, while the psychrometric chart is used to analyze the air properties. The study indicated that increasing the heat and mass transfer area of the cooling pad significantly improves the cooling efficiency of the system and also shows that by increasing the heat and mass transfer area by 20%, the cooling capacity of the system increases by 14.4%, while the power consumption increases by only 4.7%.

R. S. Bindu et al. [15] presented a detailed design and analysis of an Indirect Evaporative Cooler (IEC) of flat plate-counter flow type to optimize the IEC design for better cooling efficiency. To characterize the design of the IEC, including the heat exchanger, the water distribution system, and the air handling system, mathematical models were used to examine the performance of the IEC, which included the heat and mass transfer processes in the heat exchanger and the air streams. To characterize the design of the IEC, including the heat exchanger, water distribution system, and air handling system, mathematical models were used to analyze the performance of the IEC, which included the heat and mass transfer processes in the heat exchanger and air streams. The experimental setup was used to validate the IEC's performance, and the experiments were carried out under various operating conditions to investigate the effects of air flow rate, water flow rate, and ambient temperature on the IEC's cooling performance.

E. D. Rogdakis et al. [16] provided an overview of Maisotsenko cycle (M-cycle) technology and its potential for energy savings in cooling systems and covered the basic principles of evaporative cooling as well as the thermodynamics of the M-cycle. The M-cycle is a thermodynamic cycle that uses a cross-flow heat exchanger to improve the efficiency of evaporative cooling systems. The M-cycle and its potential for energy savings in cooling systems were theoretically examined in this research. The M-cycle was compared to a typical evaporative cooling system, and it was discovered that the M-cycle has the potential to lower cooling system energy usage by up to 30%. This paper also discussed the limitations of the M-cycle and its potential for future research and development, recommending that future research focus on optimizing the design of the heat exchanger and investigating the potential for using the cycle in conjunction with other cooling technologies.

T. Sun et al. [17] investigated the effect of water spraying in an Indirect Evaporative Cooler (IEC) from the perspective of nozzle type and spray strategy, such as intermittent spraying and continuous spraying, and the experiments were carried out on a full-scale IEC test rig with two spray systems, namely a showerhead spray system and a nozzle spray system. The results revealed that both spray systems can increase the IEC's cooling performance, with the nozzle spray system outperforming the shower head spray system. In terms of cooling effectiveness and efficiency, the continuous spraying method outperformed the intermittent spraying technique. The study defined cooling effectiveness as the ratio of temperature reduction achieved by the IEC to temperature differential between the inlet and exit air streams and it is increased as the water flow rate increased, with the nozzle spray system with continuous spraying achieving the highest cooling effectiveness of 89.3%.

Chen et al. [18] investigated the power and efficiency optimization of an Open Maisotsenko-Brayton cycle (OMBC) for power generating applications and compared it to the classic Open Regenerative Brayton cycle (ORBC). The OMBC has an indirect evaporative cooler, a compressor, a recuperator, and a turbine, but the ORBC has a direct contact evaporative cooler rather than an indirect one. Under the same operating conditions, the results revealed that the OMBC can produce a higher power output and efficiency than the ORBC. The OMBC's maximum power output was determined to be 8.8% higher than the ORBC's, while its maximum thermal efficiency was 4.4% higher. The OMBC parameters were optimized to achieve the highest power output and efficiency, and it was discovered that the optimum values of recuperator effectiveness and turbine inlet temperature were 0.8 and 603°C, respectively, with corresponding power output and efficiency of 28.5 MW and 43.5%.

M. Kheiri et al. [19] proposed a novel approach to modeling and optimizing the performance of Dew-Point Evaporative Coolers (DPECs) by proposing a GMDH-type Neural Network (GNN) model to predict the performance of DPECs based on input parameters such as outdoor air temperature, relative humidity, and dew point temperature. The model is trained with experimental data and validated with additional data. The results revealed that the GNN model accurately predicts the performance of DPECs, with a correlation coefficient of 0.99 and a mean absolute percentage error of 2.03%, and the model was used to optimize the performance of DPECs by modifying the water supply temperature and flow rate. The results also reveal that the best operating settings vary based on the external air conditions. Overall, the study provided a useful tool for designing and optimizing DPECs, which have the potential to considerably reduce energy usage in buildings.

M.H. Mahmood et al. [20] offered a thorough description of the Maisotsenko cycle, a thermodynamic cycle that combines evaporative cooling and air compression to produce very low temperatures with high efficiency, and introduced the basic concept, history, and main components of the cycle. The cycle's thermodynamic principles were introduced, and a full analysis of its performance, including its Coefficient of Performance (COP) and cooling capacity, was presented. Finally, a review of the cycle's multiple uses in industries such as air conditioning, refrigeration, and power production was presented. The paper concentrates mostly on the cycle's theoretical elements, with little information on its practical implementation or experimental confirmation. More detail on the problems and constraints of applying the cycle in real-world applications would have been helpful.

CHAPTER 3
RESEARCH GAP

A thorough literature assessment revealed the following research gaps:

- While there have been many modeling studies on the M-cycle Heat and Mass Exchanger (HMX) core design, a larger core or more cores are required to achieve the efficiency needed that results in a large system. Studies that concentrate on designing a compact HMX core with a small number are necessary for a compact system, which is scanty.

- Despite the fact that smaller M-cycle based evaporative coolers have been developed for particular applications,the scaling property of the structures is lacking.

- Studies on modeling evaporative cooling systems that concentrate on even flow distribution in HMX cores are relatively few and far between. The secondary working air and water being distributed equally in HMX cores will result in increased heat transfer, reduced fouling and reduced pressure drop.

- The majority of studies on modeling evaporative coolers employ natural cooling pads, which suit the objective of water absorption but lack the attributes of durability and reliability. There are limited experimental studies that utilize a reliable and durable cooling pad with greater water absorption.

- Research on the necessity of controllers in evaporative cooling systems is scarce. The usage of controllers can increase the efficiency of the system as well as ease the user to vary the temperature and other air-conditioning parameters via wireless technologies assisted by the controllers. This might enhance the demand for evaporative coolers in the market.

CHAPTER 4
OBJECTIVES AND METHODOLOGY

4.1. OBJECTIVES

After identifying the research gaps the prior research, the objectives of this project are as follows:

- To design a **compact structure** of regenerative cycle based evaporative cooler by reducing the number of HMX cores i.e. wet channels with reliable and durable cooling pads that increase heat transfer efficiency of the system and to fabricate a **Smart Regenerative Evaporative Cooler**

- To perform numerical analysis on the wet channel to increase the efficiency of the system by maintaining **even flow distribution**, which in turn can boost heat transfer, reduce fouling and reduce pressure drop.

- To develop a **controller circuit** for varying the output temperature and humidity of the system by varying the inlet flow rate using a wireless technology.
  - Temperature - 22℃ to 27℃
  - Relative humidity (RH) - 40% to 60%

4.2. METHODOLOGY

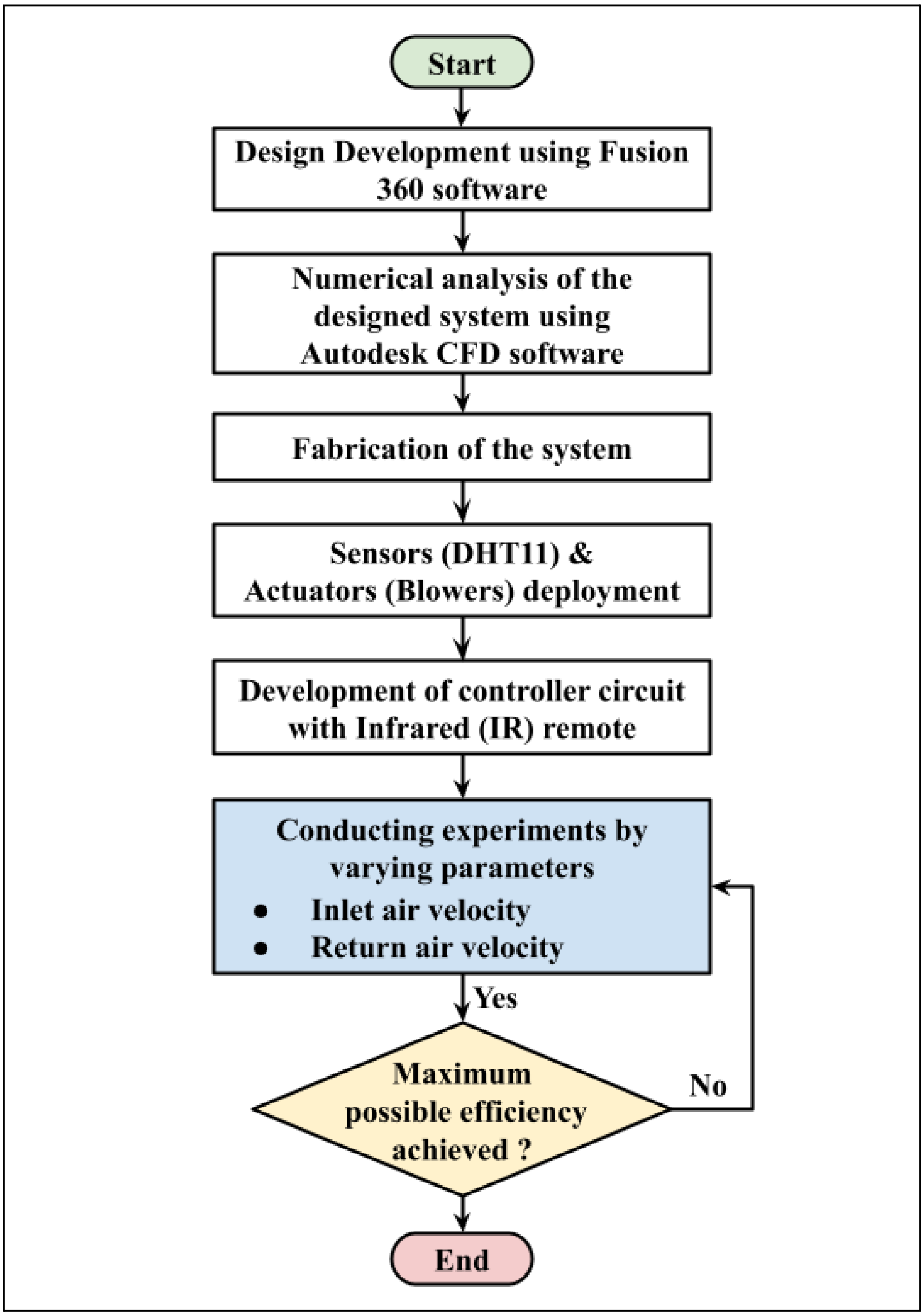

Fig. 4.1. Methodology

CHAPTER 5
NUMERICAL ANALYSIS OF
WET CHANNEL FOR UNIFORM FLOW DISTRIBUTION

5.1. DESIGN OF THE GEOMETRY

An important aspect of the system's design is the radial arrangement of the tubes as in figure 5.1 in the wet channel. The main objective of this configuration is to maintain even flow distribution in the wet channel. The tubes are arranged in a circular pattern in which a cooling pad is positioned in the middle of each tube. This maximizes the cooling pad's surface area in contact with the air stream by ensuring that the entire cooling pad is equally moistened. Greater heat transfer between the air and the water as a result of the higher contact area results in more effective cooling.

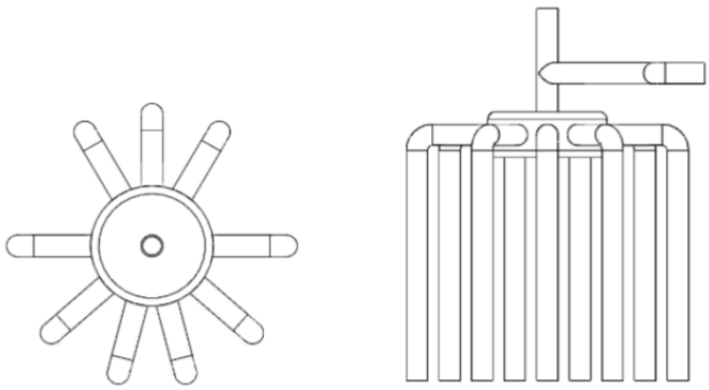

Fig. 5.1.1. Top view with radial arrangement of tubes

Fig. 5.1.2. Front view with proper pitching of tubes

Fig. 5.1. Design of the geometry

The design ensures proper pitching of the tubes in the wet channel as shown in figure 5.1 is critical to achieve higher contact between the dry air and the wet channel. The radial arrangement of the tubes is beneficial, as it provides even flow distribution across the wet channel. However, it is important to ensure that the tubes are not inline and that they are pitched at an appropriate angle to maximize contact between the dry air and the surface of the wet channel.

5.2. NUMERICAL FLOW ANALYSIS

This numerical simulation is based on the laws of continuity and momentum conservation, which is governed by the following equations:

Continuity equation:

$$\frac{\partial \rho}{\partial t} + \frac{\partial \rho u}{\partial x} + \frac{\partial \rho v}{\partial y} + \frac{\partial \rho w}{\partial z} = 0 \qquad \text{.... (5.1)}$$

MOMENTUM EQUATIONS

X-Momentum equation:

$$\rho\frac{\partial u}{\partial t} + \rho u\frac{\partial u}{\partial x} + \rho v\frac{\partial u}{\partial y} + \rho w\frac{\partial u}{\partial z}$$

$$= \rho g_x - \frac{\partial p}{\partial x} + \frac{\partial}{\partial x}\left[2\mu\frac{\partial u}{\partial x}\right] + \frac{\partial}{\partial y}\left[\mu\left(\frac{\partial u}{\partial y} + \frac{\partial v}{\partial x}\right)\right] + \frac{\partial}{\partial z}\left[\mu\left(\frac{\partial u}{\partial z} + \frac{\partial w}{\partial x}\right)\right] \qquad \text{.... (5.2)}$$

$$+ S_\omega + S_{DR}$$

Y-Momentum equation:

$$\rho\frac{\partial v}{\partial t} + \rho u\frac{\partial v}{\partial x} + \rho v\frac{\partial v}{\partial y} + \rho w\frac{\partial v}{\partial z}$$

$$= \rho g_y - \frac{\partial p}{\partial y} + \frac{\partial}{\partial x}\left[\mu\left(\frac{\partial u}{\partial y} + \frac{\partial v}{\partial x}\right)\right] + \frac{\partial}{\partial y}\left[2\mu\frac{\partial v}{\partial y}\right] + \frac{\partial}{\partial z}\left[\mu\left(\frac{\partial v}{\partial z} + \frac{\partial w}{\partial y}\right)\right] \qquad \text{.... (5.3)}$$

$$+ S_\omega + S_{DR}$$

Z-Momentum equation:

$$\rho\frac{\partial w}{\partial t}+\rho u\frac{\partial w}{\partial x}+\rho v\frac{\partial w}{\partial y}+\rho w\frac{\partial w}{\partial z}$$
$$=\rho g_z-\frac{\partial p}{\partial z}+\frac{\partial}{\partial x}\left[\mu\left(\frac{\partial u}{\partial z}+\frac{\partial w}{\partial x}\right)\right]+\frac{\partial}{\partial y}\left[\mu\left(\frac{\partial v}{\partial z}+\frac{\partial w}{\partial y}\right)\right]+\frac{\partial}{\partial z}\left[2\mu\frac{\partial w}{\partial z}\right] \quad \ldots .(5.4)$$
$$+S_{\omega}+S_{DR}$$

The two source terms in the momentum equations are for rotating coordinates and distributed resistances respectively.

The distributed resistance term can be written in general as:

$$S_{DR}=-\left(K_i+\frac{f}{D_H}\right)\frac{\rho V_i^2}{2}-C\mu V_i \quad \ldots .(5.5)$$

where i refers to the global coordinate direction (u, v, w momentum equation) and the other terms are described in the previous section.

Note that the K-factor term can operate on a single momentum equation at a time because each direction has its own unique K-factor. The other two resistance types operate equally on each momentum equation. The other source term is for rotating flow.

The rotating flow term can be written in general as:

$$S_{\omega}=-2\rho\omega_i\times V_i-\rho\omega_i\times\omega_i\times r_i \quad \ldots .(5.6)$$

The flow through the wet channel is analyzed to validate the even flow distribution of fluid for the developed design. The software used is Autodesk CFD, which uses Computational Fluid Dynamics (CFD) to simulate the flow of air and water through the system, and to predict the performance of the system under different operating conditions.

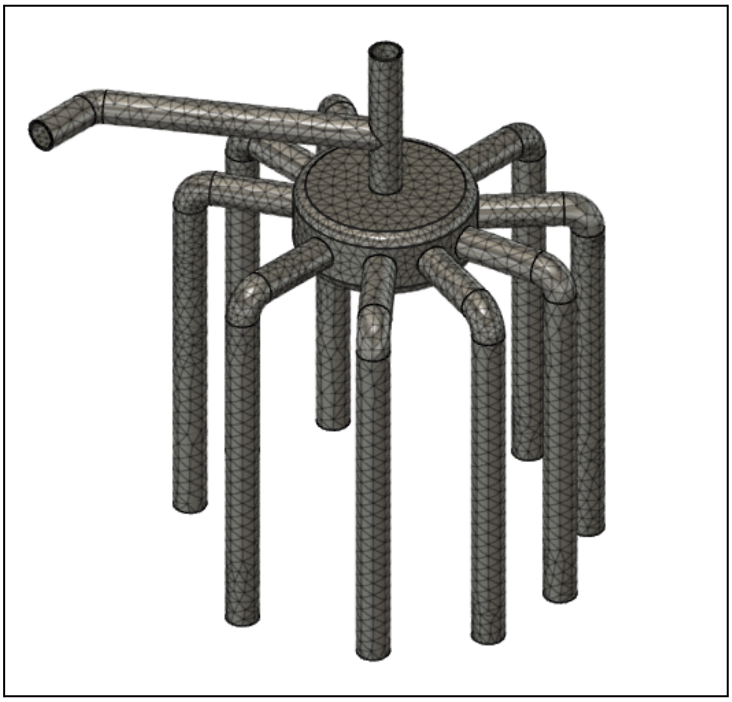

Fig.5.2. Mesh of the computational domain

With the help of Autodesk CFD software and staggered mesh grids, the finite element method, Tri Diagonal Matrix Algorithm (TDMA) and k-ε model are used to solve and the solver used is segregated solver in which each of the dependent variables are solved separately. The fluid in the geometry is set to be incompressible and the flow of the fluid is set to be turbulent. The matrix equation for TDMA can be written as:

$$A_{i-1,j}\phi_{i-1} + A_{i,j}\phi_{i-1} + A_{i+1,j}\phi_{i+1} = \sum_{j \neq i-1, j \neq i, j \neq i+1} A_{i,j}\phi_j + F_i \qquad \textbf{.... (5.7)}$$

The surface refinement is enabled and the gap refinement is disabled for creating mesh of the geometry. The mesh of the geometry is autosized with the scale length of 0.4598 which creates a count of 1,30,903 mesh elements.

Geometry description	Material	Boundary conditions (Inlet conditions)
Channel surface	Copper	• Thickness - 1 mm
Fluid at the top of the channel	Water	• Velocity - 3.88 m/s • Pressure - 7 Kpa
Fluid at the side of the channel	Air	• Velocity - 25 m/s • Pressure - 11 KPa

Table 5.1. Simulation boundary conditions

A study was conducted to investigate the characteristics of a designed geometry that involved copper tubes. Water was selected as the medium for this study, and the study was conducted under ambient climatic conditions. To analyze the flow distribution, the study established inlet and outlet boundary conditions for the geometry. The inlet boundary condition considered the water's pressure and velocity, with the velocity being computed to be 3.88 m/s and pressure 7 kPa. The outlets of the tubes were considered to be zero gradient. To ensure accurate meshing of the surfaces, the study refined the surface of the geometry. Auto size meshing was employed to generate a mesh for the geometry surfaces. The simulation was then solved for the velocity contour.

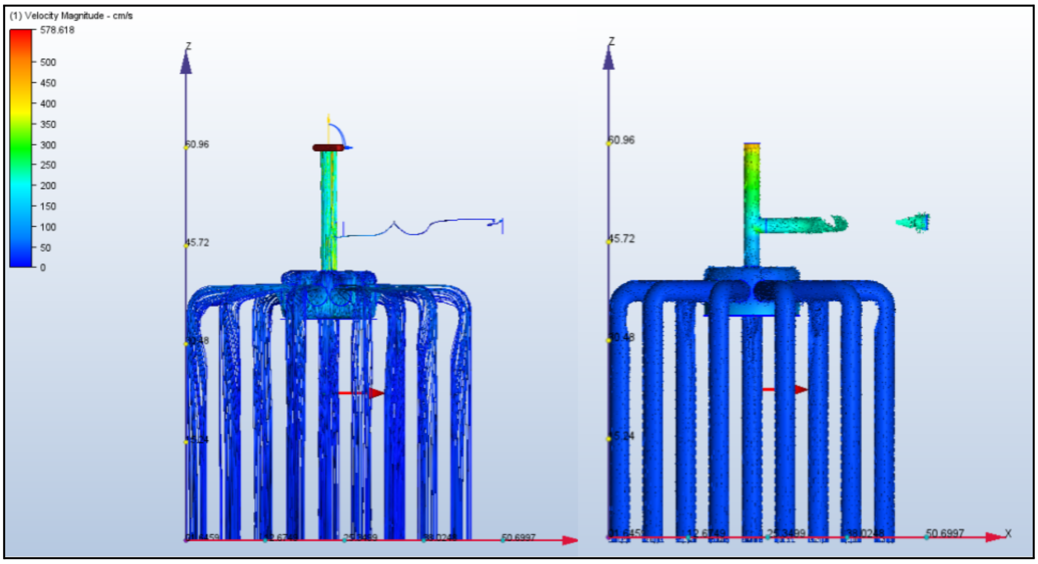

Fig. 5.3. Velocity vector contour

The simulation results show the flow distribution throughout the geometry. The trace vector flow of the findings, which gives outlines of a flow, can be used to obtain the velocity at each tube end.

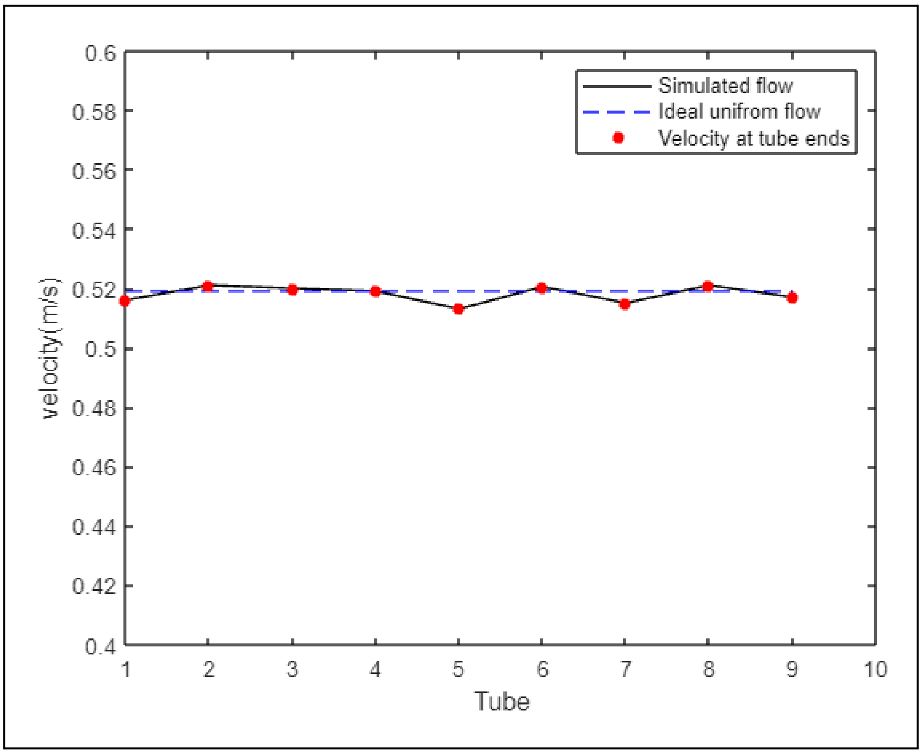

Fig. 5.4. Velocity of fluid in each tube outlet

The graph plotted by the results is displayed in figure 5.4 that describes the behavior of the fluid. The velocity of fluid from each tube is approximately 0.5 m/s which varies with corresponding inlet velocity. The uniformity of the fluid's velocity in each tube, which is readily apparent, confirms that the established design of the wet channel can achieve an even distribution of fluid through the tubes.

CHAPTER 6
DESIGN DEVELOPMENT

6.1. PRODUCT LAYOUT

The layout of the system depicted in figure 6.1 describes a system consisting of a cooling system sandwiched between a tank and a reservoir, with both the tank and the reservoir filled with water that is continually circulated throughout the system by a pump. The cooling system includes a cooling pad that the water flows across continuously, resulting in evaporation and cooling of the air passing through the pad.

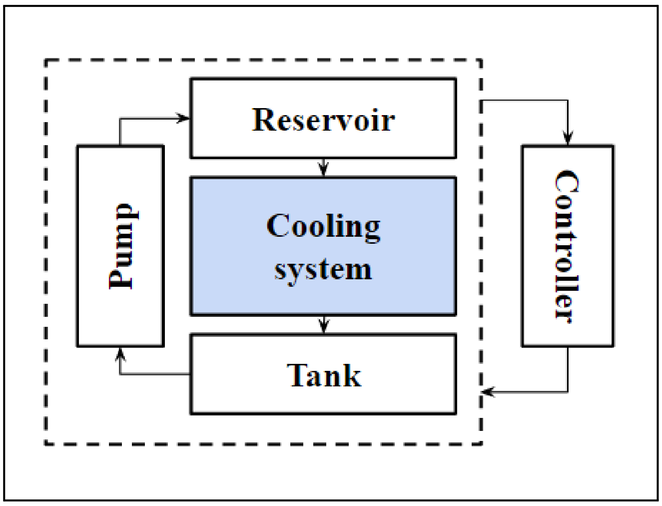

Fig. 6.1. Block diagram of the system

One important aspect of the system is the presence of a controller which continuously monitors the water level of the system and provides an indication if the water level is lower than a reference level. This is a crucial feature as evaporative cooling systems rely on the presence of water in the system for their operation, and a low water level can result in reduced cooling performance or even system failure.

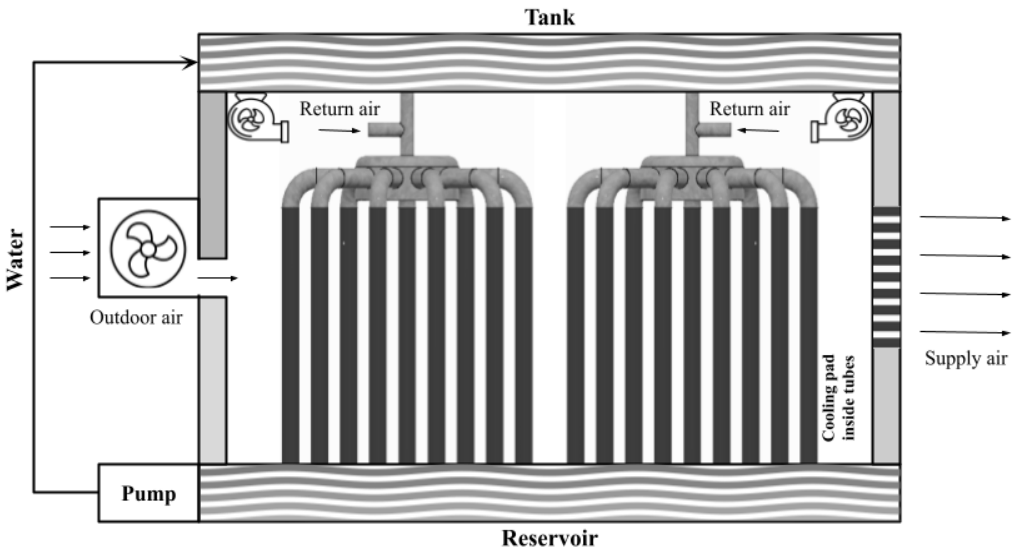

fig. Schematic diagram of designed Regenerative Evaporative Cooling system

The cooling system of the product relies on regenerative evaporative cooling, which boosts cooling effectiveness by using a heat exchanger and return air stream. Typical parts of a regenerative evaporative cooler are a dry channel, heat exchangers or wet channels, a water pump, a water distribution system, a fan, and a controller. The incoming outdoor air is directed towards the wet channel where it is cooled by transferring heat to the outgoing air to begin the process of a Regenerative Evaporative Cooler. The cooled air is divided into supply and return air. The area that has to be cooled receives the supply air whereas the return air along with the water is recirculated to the wet channels. The water distribution system receives the warm, humid outgoing air, which is then cooled by water evaporation there.

The controller continuously monitors temperature, humidity, and water level which in turn activates the pump to refill the system when the water level falls below a specified threshold. Even water distribution throughout the cooling pad is essential for efficient cooling since uneven distribution causes dry areas, lowering overall efficiency.

6.2. DESIGN IMPROVEMENT

Using Autodesk Fusion 360 software, a 3-Dimensional Computer Aided Design (CAD) model of the system is developed in order to visualize the finished product and simulate the working of the model using numerical analysis. The new ideologies developed throughout the design development process are used to improve the design. The design has been updated for greater performance, and it is expected to be more effective than the previous design.

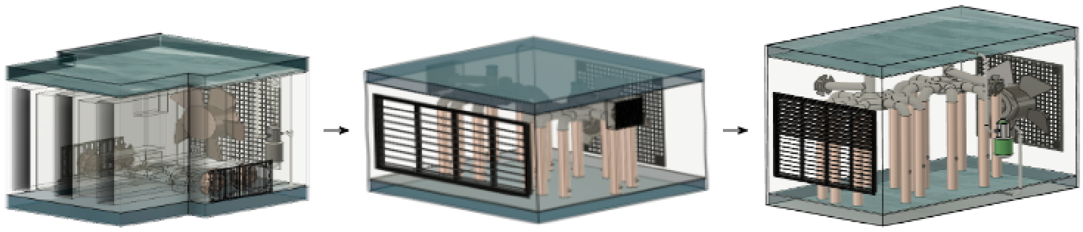

Fig. 8.1. Design 1 Fig. 8.2. Design 2 Fig. 8.3. Design 3

Fig. 6.3. Design improvement

The design 1 in figure 6.3 was developed by applying the fundamental ideologies of the regenerative evaporative cooling system that demands air regeneration. The wet channels are configured so that each wet channel is sandwiched between the dry channels on either side for greater heat transfer. The path beneath the channels is provided to isolate the return air from the dry channel while allowing it to circulate throughout the wet channel. Convective heat transfer occurs between the wet channel walls and the air stream in the dry channel, resulting in a supply air stream with lower temperature and humidity.

The plate arrangement did not adequately address issues with flow distribution as the wet channels at the edges receive maximum flow whereas the central channels receive comparatively less. As a result, the design 2 in figure 6.3 is developed with an optimized wet channel by considering even flow distribution, increasing the efficiency of heat transfer. In design 3 in figure 6.3, the horizontal configuration of wet channels is changed to vertical, which increases heat transfer by lengthening the air passage.

6.3. MODEL DESCRIPTION AND MATERIAL SELECTION

6.3.1. COOLING PAD - MATERIAL ANALYSIS

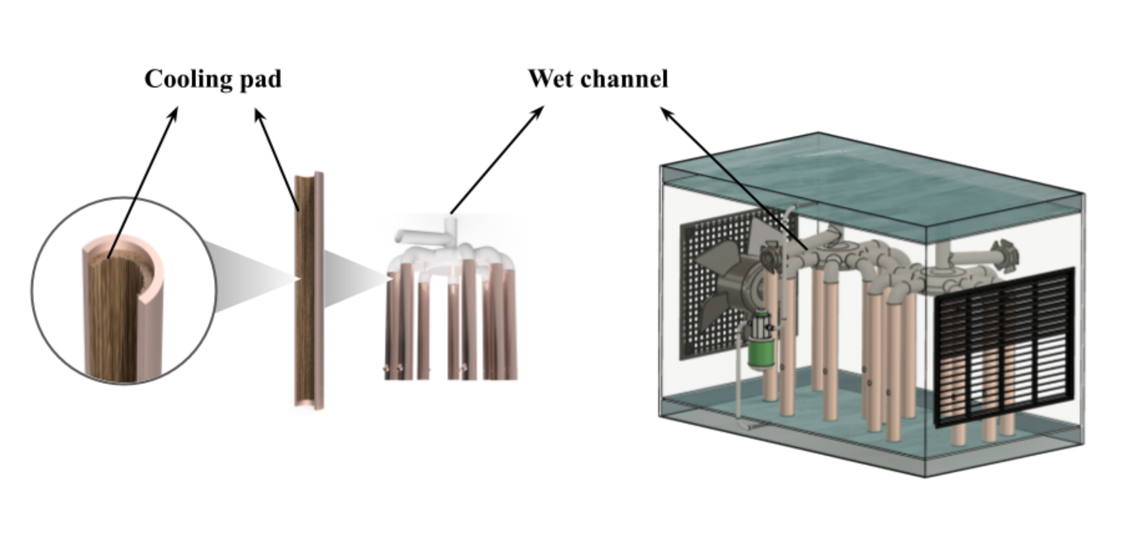

Fig. 6.4. Cooling pad position

The cooling pads are placed inside the tubes of the wet channel where it is inserted at the edges of the tube. By positioning the pads at the edges, provision for air flow can be made inside the tube. The table 6.1 presents the types of cooling pads and their scopes for usage.

COOLING PAD	POSITIVES	NEGATIVES
Aspen wood fiber	Resist deterioration by water and sunlight	Susceptible to bacteria and mildew
Cellulose	Highly efficient	Not durable and reliable
Other natural fibers	High water absorption	Not durable and reliable
PVC and synthetic fibers	Long lifespan and require little maintenance	Comparatively less efficient and high cost

Table 6.1. Analysis of cooling pads through literature review

- <u>Material</u> - **Hydrophilic polypropylene**

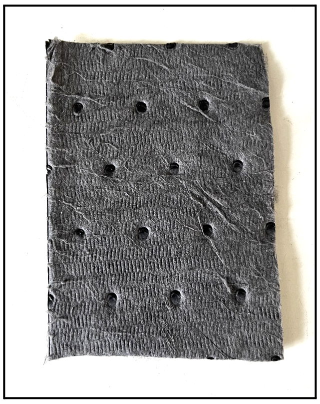

Fig. 6.5. Hydrophilic polypropylene material

Though synthetic fibers fall short of natural cooling pads in water absorption it can, however, be treated in order to become hydrophilic in nature. The cooling pad material of choice is hydrophilic treated polypropylene which is shown in figure 6.5.

6.3.2. MAJOR COMPONENTS OF THE SYSTEM

To virtually represent the ideologies created for the project, a CAD model was created. The design is made transparent for easy visualization. The components of the design are as follows:

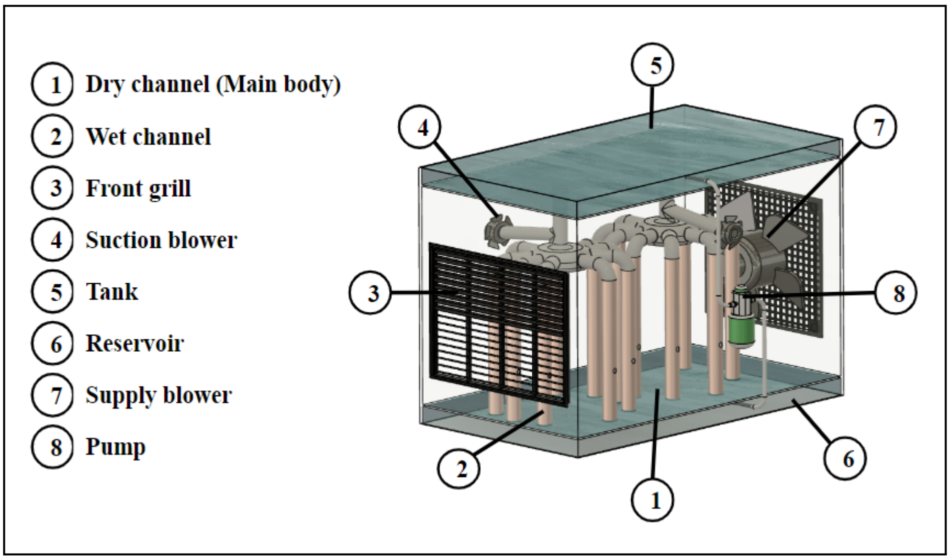

Fig. 6.6. Components of the design

1. **Dry channel:**

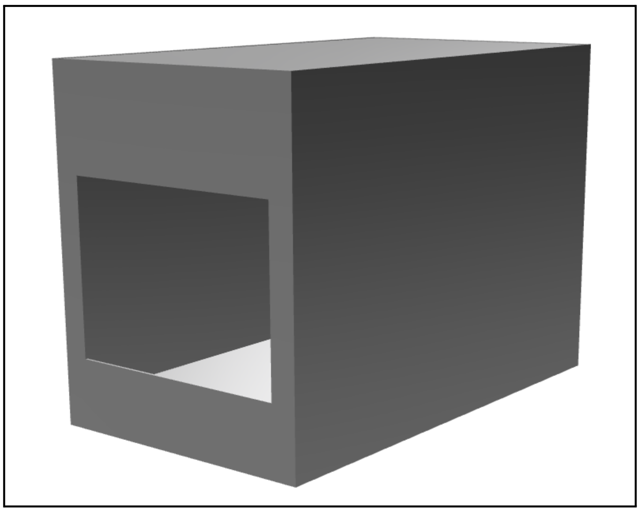

Fig.6.7. Dry channel

a. **<u>Material</u> - Stainless steel**

b. Due to its excellent strength-to-weight ratio, resistance to corrosion, machinability, availability, high durability, and low thermal conductivity, stainless steel is used for the dry channel of evaporative coolers.

c. The dry channel should have low thermal conductivity so that there is minimal transfer of heat between the system and the environment as they use water evaporation to cool the air around them.

d. Another reason for using this material to construct the system's frame is that it can withstand moisture and high humidity, which can cause corrosion and rust in other materials.

e. Furthermore, stainless steel is simple to clean and maintain, extending the cooler's lifespan.

2. **Wet channel:**

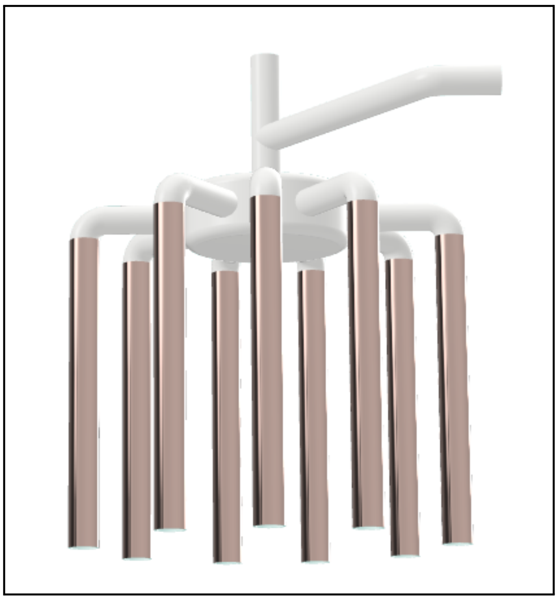

Fig.6.8. Wet channel

a. **<u>Material</u> - Copper**

b. Copper is primarily used to construct wet channels of the evaporative cooler due to its great thermal conductivity, which makes it a very efficient material for heat transfer.

c. The ability of copper to withstand corrosion is essential for the cooler's durability and reliability. Additionally, copper has properties such as strength-to-weight ratio, resistance to corrosion, machinability, availability and high durability.

d. Copper has a relatively high specific heat capacity, which means that it can absorb a lot of heat energy without experiencing a large temperature increase so that the temperature of the air stream will not be increased.

3. **Front grill**
    a. The front grill serves as a safeguard for the internal parts, which shut the supply air entrance while allowing air into the interior space.

4. **Suction blower**
    a. A pair of suction blowers installed at the horizontal opening of each wet channel allows return air to flow through the wet channel, allowing water in the cooling pad to evaporate.
    b. This regeneration of air to the wet channel leads to enhanced heat transfer and can increase cooling efficiency gradually over time.

5. **Tank**
    a. The tank of the system stores water at the top and allows water to flow through the wet channel due to gravity.

6. **Reservoir**
    a. The reservoir collects the water that drains from the wet channel after the saturation of cooling pads.

7. **Supply blower**
    a. The supply blower draws in external air and directs the stream of air into the dry channel, where half of it is given to the space after being cooled by the wet channels which is the supply air and the other part is regenerated into the wet channel which is the return air.

8. **Pump**
    a. The flow of water from the reservoir to the tank is achieved by the pump.
    b. By allowing the water to flow into the tank, the water collected in the reservoir from the wet wet channel is recycled with the help of the pump.

6.4. DESIGN DIMENSIONS

The design of the product is essential for its optimal performance, and the dimension of the assembly plays a crucial role in achieving this. The product in Figure 6.9 is designed to fit the space decided to place the product. The entire dimensions of the product is 20 x 40 x 28 inches. The blower opening in the dry channel has a diameter of 12 inches, which allows for efficient air intake. The front grill opening, with dimensions of 12 x 18 inches, facilitates the flow of air into the system. The tank and the reservoir are designed with a height of 2 inches each to hold water for the cooling process. The dry channel has a height of 26 inches to let the air flow inside the system for heat exchange.

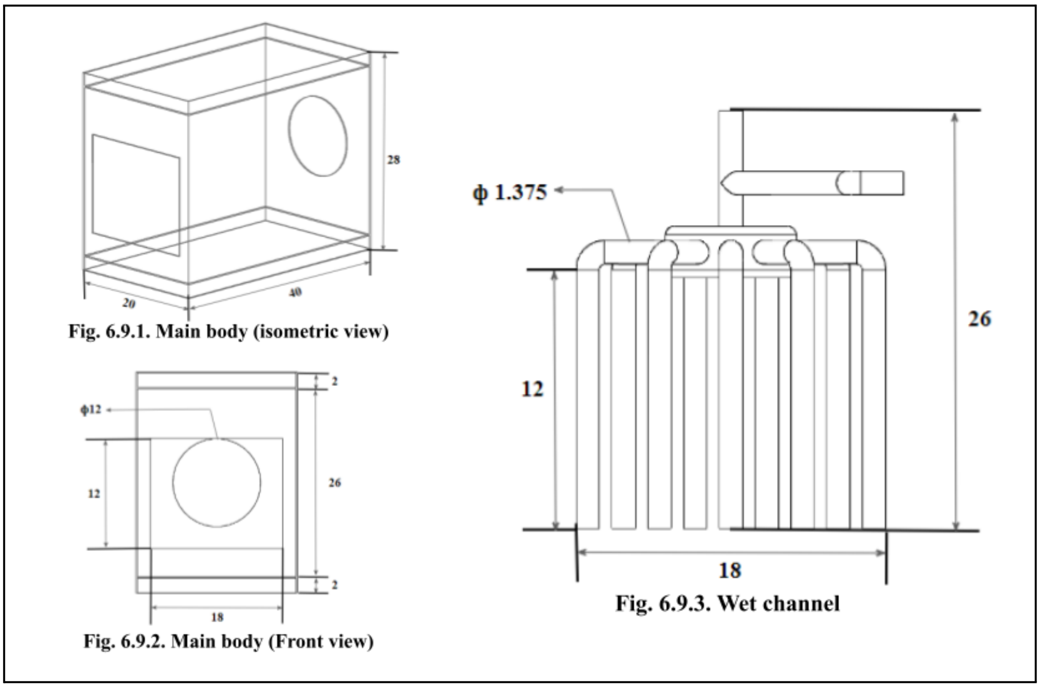

Fig. 6.9.1. Main body (isometric view)
Fig. 6.9.2. Main body (Front view)
Fig. 6.9.3. Wet channel

Fig. 6.9. Dimensions of the product in inch

The wet channel, on the other hand, has an overall height of 26 inches and a radius of 18 inches, with a length of 12 inches for each tube. The cooling pads, which are inserted into tubes with a diameter of 1.375 inches, facilitate the cooling process. These design elements work together to create an effective cooling system.

CHAPTER 7

FABRICATION OF EXPERIMENTAL SETUP

7.1. DRY CHANNEL FABRICATION

The dry channel of the system is a critical component and in order to ensure optimal performance of the system, it is important to design and fabricate the dry channel with precision and attention to detail.

Fig. 7.1.1. Sheet cutting

Fig. 7.1.2. Sheet bending

Fig. 7.1. Sheet machining

After selecting a stainless steel material, the sheet is cut to the desired size and shape using a variety of machining processes such as sawing and cutting. The sheets are then bent as in figure 7.1.2 to increase their strength and ease of assembly.

Fig. 7.2. Sheet welding

The next step in the fabrication process is to weld or bolt the individual bent sheets together to form a complete channel as in figure 7.2.

Fig. 7.3. Tank of the system

The tank and the reservoirs are also made through the same processes with respect to the dimensions of the dry channel.

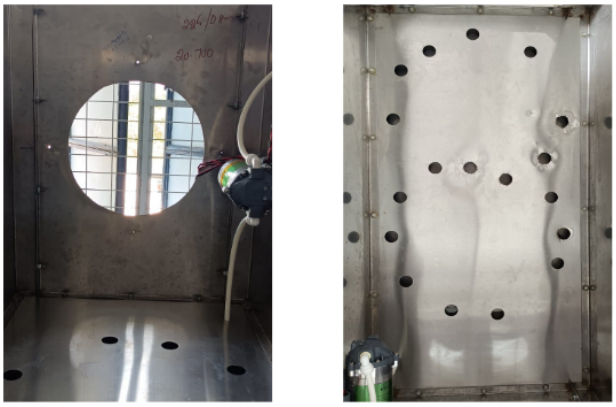

Fig. 7.4.1. Blower provision **Fig. 7.4.2. Wet channel provision**

Fig. 7.4. Provisions in the dry channel

Finally, the provisions for the front grill, blower, the pump and the wet channels are provided. The base of the dry channel is bored using hole saw as in figure bit for preventing moisture in the dry channel.

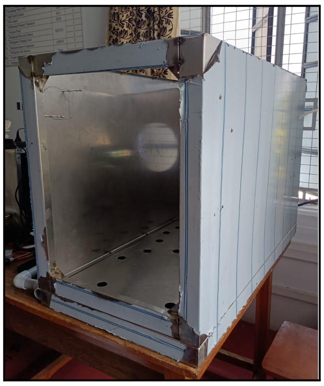

Fig. 7.5. Fabricated dry channel

7.2. WET CHANNEL FABRICATION

Copper is used as a material for fabricating the wet channel due to its excellent thermal conductivity and its ability to resist corrosion. To fabricate the wet channel using copper, the tubes are first cut to the required length using cutting tools.

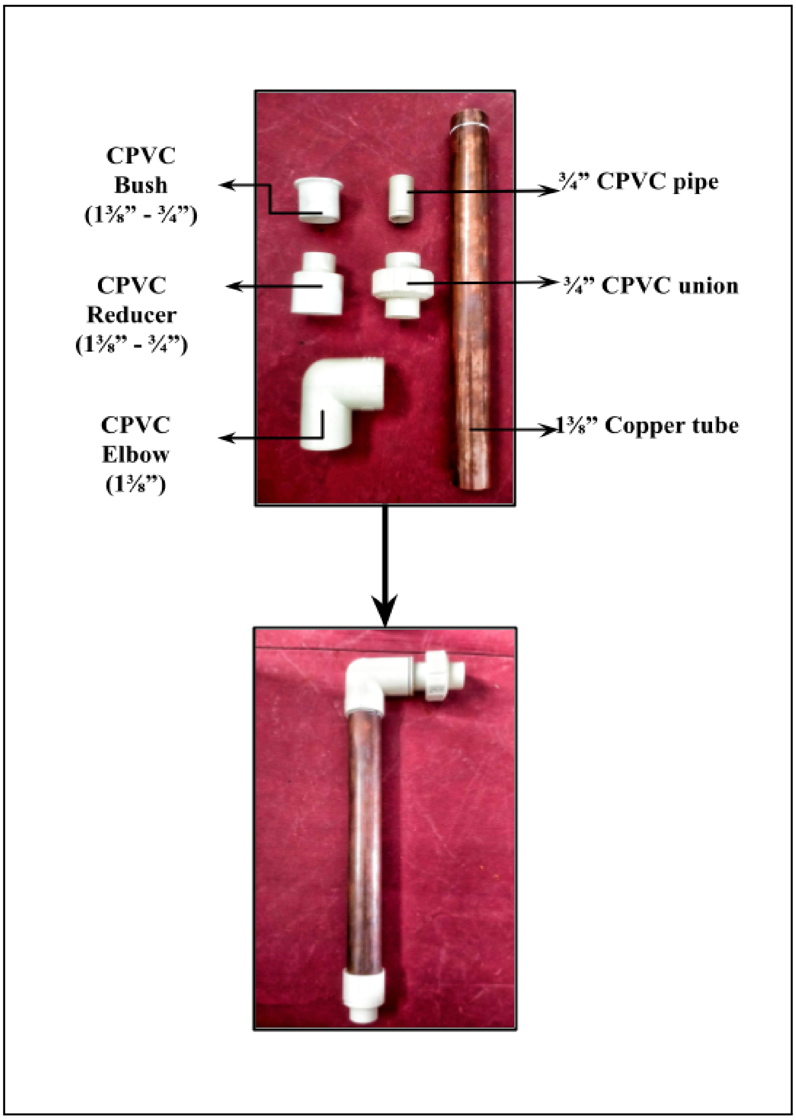

Fig. 7.6. Wet channel tube assembly

CPVC pipes and other accessories such as bush, reduser, elbow and union are assembled together to form a single tube. The hollow copper tube is filled with hydrophilic polypropylene material which is already used.

The header of the wet channel shown in figure 7.7.1 is designed in such a manner that the water is entered to the center of the channel. The header is assembled using PVC and CPVC accessories. The holes in the header are drilled with the designed angle for proper pitching and hence, it can be properly staggered for maximum contact area between the dry channel airstream and the wet channel surface.

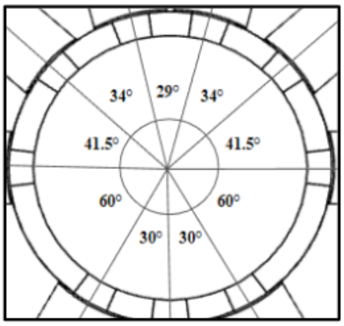

Fig. 7.7.1. Angles of the drill

Fig. 7.7.2. Assembled header

Fig. 7.7. Header of the wet channel

The provisions for the air and water flow are provided at the side and the top of the headers respectively. Then, the header is sealed completely to prevent the leakage. Finally, the header and tubes are connected to form a wet channel as in figure 7.8.

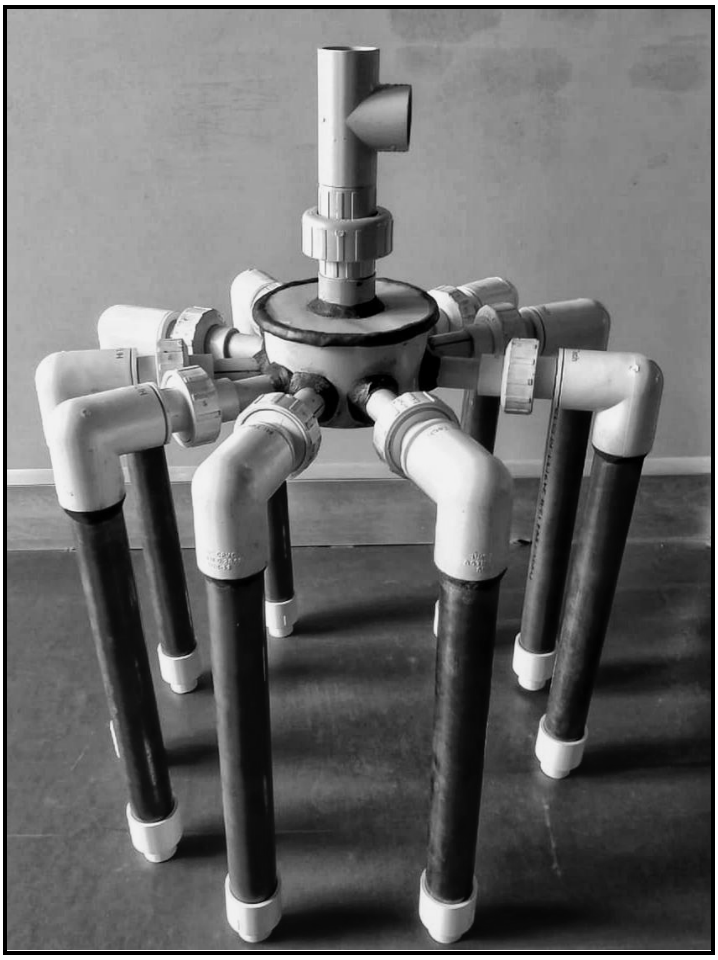

Fig. 7.8. Fabricated wet channel

7.3. FINAL ASSEMBLY

The supply blower is installed at the back of the system where the provision is made in the dry channel. The pump and the controller circuit are located at the left and the right of the system respectively.

Fig. 7.9. The front grill

The front grill is made of stainless steel and is designed to deliver air to the space as well as protect the inner components. It is located at the front of the system in the dry channel provision.

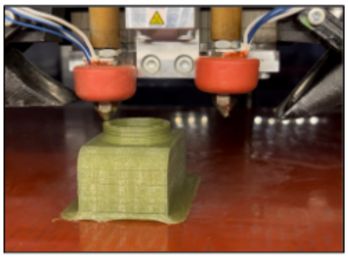

Fig. 7.10.1. 3D printing

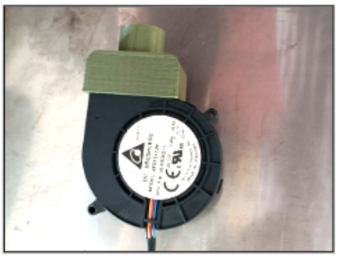

Fig. 7.10.2. Blower with the component

Fig. 7.10. 3D printed component

The suction blowers are installed at either side of the wet channels on the walls of the system. The suction blower is connected to the wet channel by using PVC pipes and a 3D printed component. The 3D printed component is shown in figure 7.10.1 and it is designed using Fusion 360 software.

Finally, all the components are assembled to form a complete system. Experimental analysis can be conducted using the setup by varying the speed of the supply and the suction blowers. The complete experimental setup is shown in figure 7.11.

Fig. 7.11.1. Right perspective view

Fig. 7.11.2. Left perspective view

Fig. 7.11.3. Front view

Fig. 7.11.4. Back view

Fig. 7.11. Regenerative Evaporative Cooler setup

7.4. SUPPLY BLOWER CONTROLLER

7.4.1. CIRCUIT DIAGRAM

The controller circuit for the supply blower is designed using ATMega328P microcontroller and it is designed for 3 different speeds. The figure 7.12 shows the circuit diagram of the controller circuit.

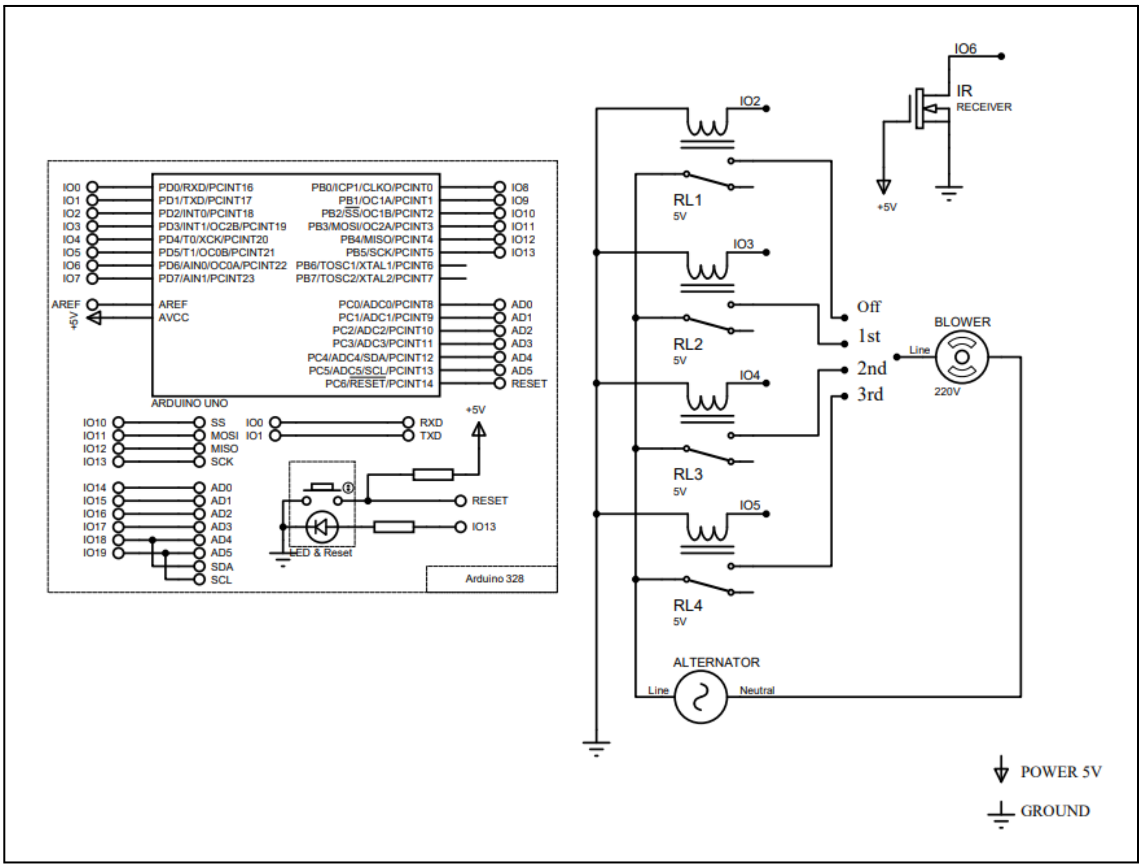

Fig. 7.12. Circuit diagram of supply blower controller

To make the controlling easier, the IR sensor module is used in which the receiver is connected to the circuit whereas the transmitter is held by the user. The controller code is attached to the Appendix A.

7.4.2. CIRCUIT COMPONENTS AND CONNECTION

The components of the circuit includes ATmega controller (Arduino UNO) for establishing programming code, IR receiver module for receiving data from IR transmitter and 4 channel relay module for switching operations.

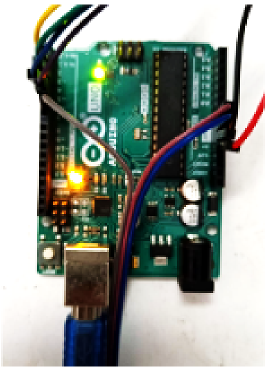
Fig. 7.13.1. Arduino controller

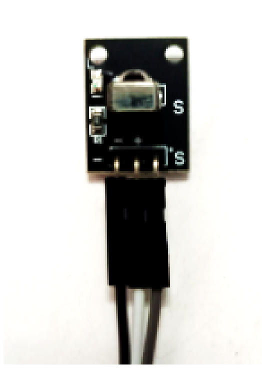
Fig. 7.13.2. IR Receiver

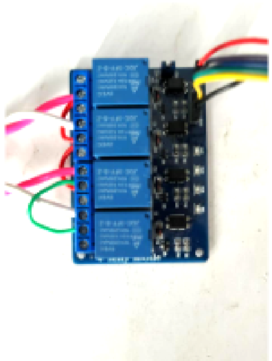
Fig. 7.13.3. 4 channel Relay module

Fig. 7.13. Components of supply blower controller

The connections of the circuit are made through connecting wires and the output of the relay module is connected to the supply blower in which each relay in the module is connected to a specific speed connection. The relay is switched with respect to the IR receiver data. The controller circuit is shown in figure 7.14.

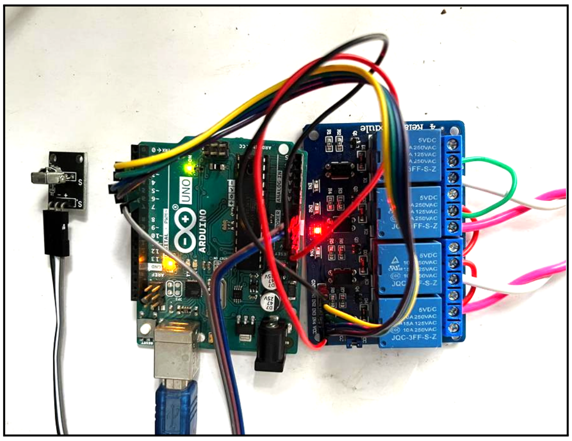

Fig. 7.14. Supply blower controller circuit

7.5. SUCTION BLOWER CONTROLLER

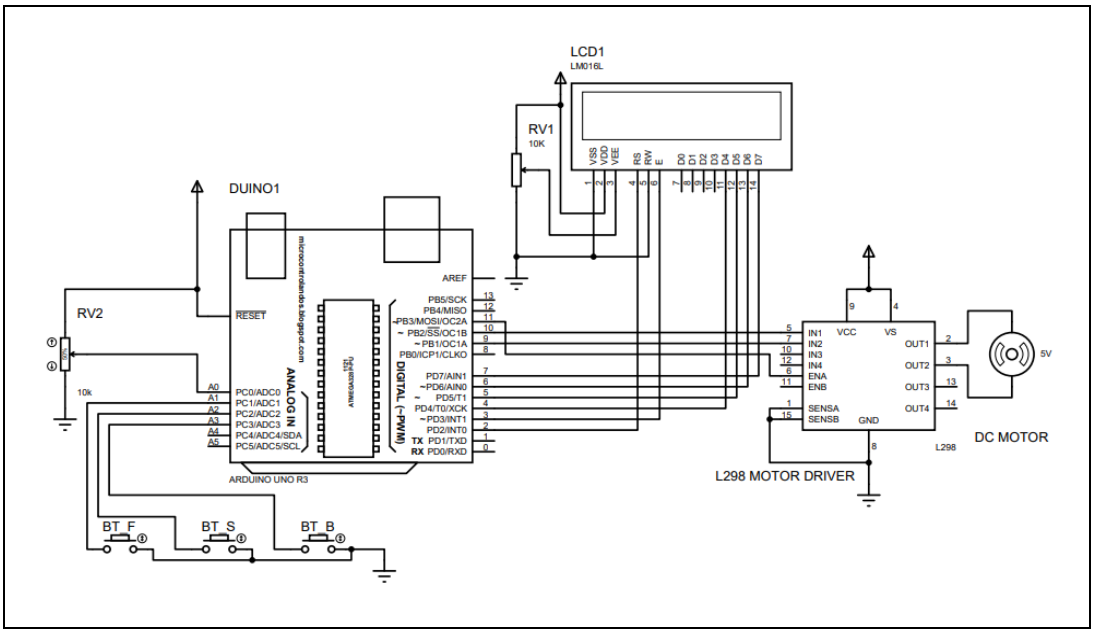

Fig. 7.15. Circuit diagram of suction blower controller

The controller of specification of 12V and 10A is connected to the suction of blowers as the rated voltage and current of each suction blowers is 12V and 3A respectively. Therefore, a 10A controller is used. Additionally, the blower can also be controlled using Pulse Width Modulation (PWM) using the ATMega328P controller.

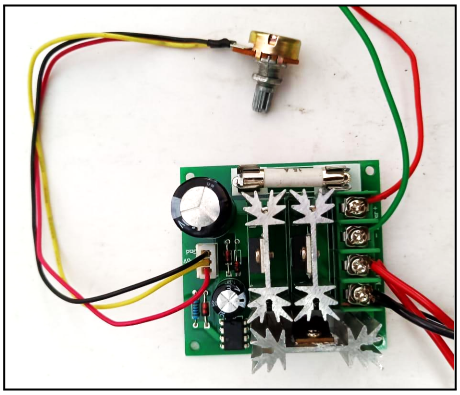

Fig. 7.16. Suction blower controller

Unlike the previous controller, this controller can vary the speed of the blower at a wider range by making use of either potentiometer or PWM by the controller. The controller code is attached to the Appendix B.

7.6 EXPENSE

SI. No	Details of Expenses	Amount in Rs
1	3/4" CPVC Pipe	4,854.00
	1" PVC Union	
	1 1/4" CPVC Elbow	
	1 1/4" x 3/4" CPVC Bush	
	4" PVC End Cap	
	1 1/4" x 3/4" CPVC Reducer	
	100ml CPVC Paste	
	3/4" CPVC UNION	
	1 1/4" x 1" PVC Bush	
2	1 3/8" HARD COPPER PIPE 20SWG 10FT	5,878.00
3	100GM M-SEAL	210.00
	MYTLOK 743 -20GM	
4	PVC End Cap Drill Machining	802.00
5	M-SEAL	75.00
	1 1/4" X 1" Reducer	
	1" Pipe	
6	Compact Rotary Fan	2,121.00
7	COSMOS SPRAY PAINT BLACK 400ML	250.00
8	COSMOS SPRAY PAINT BLACK 400ML	500.00
9	S.S. Sheet 304 8x4 N4 PVC 0.8	3,445.00
10	S.S. Sheet 304 8x4 N4 PVC 0.8	3,346.00
11	SS 304 N4 - SHEET PVC Matt JSL	3,395.00
12	SS 304 N4 - SHEET PVC Matt JSL	3,750.00
13	IR Remote	177.00
14	COIN Battery 2023	120.00
15	REES52 Motor Pump Speed Controller	2,200.00
	DEMEANOR Universal Absorbent	
16	TAPARIA BIM HOLE SAW-HSM30	289.00
17	TAPARIA BIM HOLE SAW-HSM30	289.00

18	PGSA2Z 8300 RPM Brushless Air Cooling Blower Fan	3,100.00
	12V 2A Voltage Regulator 24W DC Fan Speed Controller	
	5A 90W Voltage Regulator PWM 12V DC Motor Speed Controller	
19	BOOSTER PUMP	1,652.00
	RO TUBE 1/4	
20	Orient 450mm TORNADO-II P/F-BLACK	3,835.00
21	1" PVC Elbow	236.00
	1" PVC Pipe	
	m-Solvent	
22	12V/2.5A Adapter	590.00
23	LABOUR	8,000.00
24	L298N 2A Based Motor Driver Controller Board Module	390.00
25	OTHERS	1,300.00
26	24V/10A DC ADAPTER	1,144.60
TOTAL		**51,948.60**

CHAPTER 8
EXPERIMENTATION AND RESULTS

8.1. VARYING THE SUPPLY BLOWER FLOW RATE

Flow rate (m^3/hr)	DBT (℃)			WBT (℃)		DP (℃)		RH (%)	
	Inlet	**Outlet**	**ΔDBT**	**Inlet**	**Outlet**	**Inlet**	**Outlet**	**Inlet**	**Outlet**
2000	31.0	30.2	**0.8**	26.6	26.1	24.8	24.5	69.8	71.8
	31.9	30.8	**1.1**	26.6	26.2	24.5	24.4	65.2	68.4
	32.0	31.4	**0.5**	26.4	26.2	24.3	24.2	64.2	65.4
2300	31.6	31.3	**0.3**	26.0	26.2	23.8	23.9	63.5	64.4
	32.2	30.2	**2.0**	26.6	26.1	26.0	24.5	69.8	71.8
	33.0	31.2	**1.8**	26.9	26.3	24.6	24.5	61.7	64.5
2600	32.6	31.0	**1.6**	26.8	26.2	24.6	24.4	62.9	68.0
	32.7	31.5	**1.2**	26.4	25.8	24.0	23.6	60.3	63.3
	33.1	30.6	**2.4**	26.6	26.4	24.7	24.7	62.6	67.1

Table 8.1. Experiments by varying supply blower flow rate

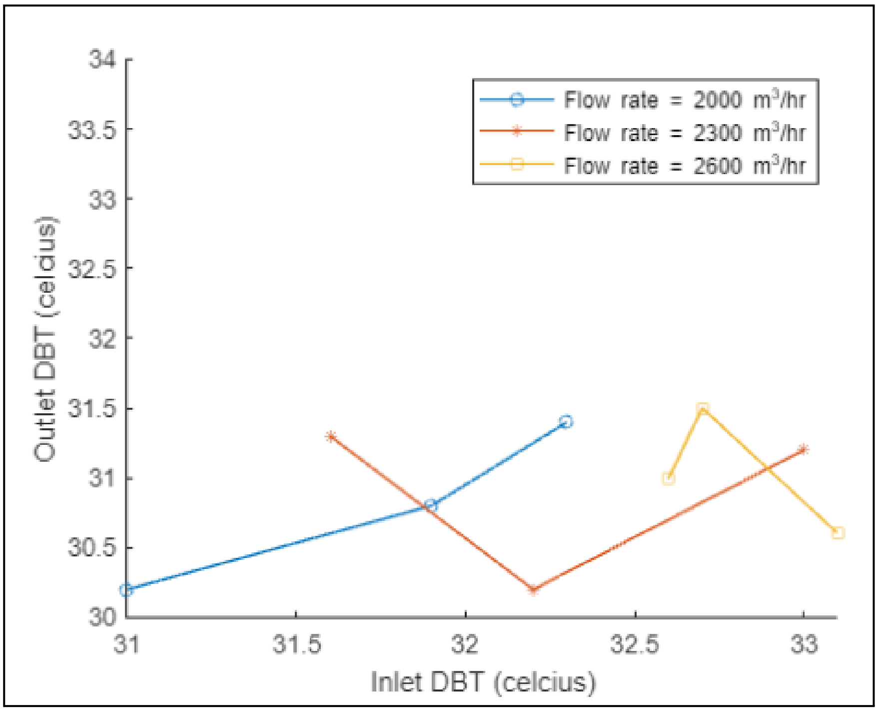

Fig. 8.1. Experiments on DBT with varying supply flow rate

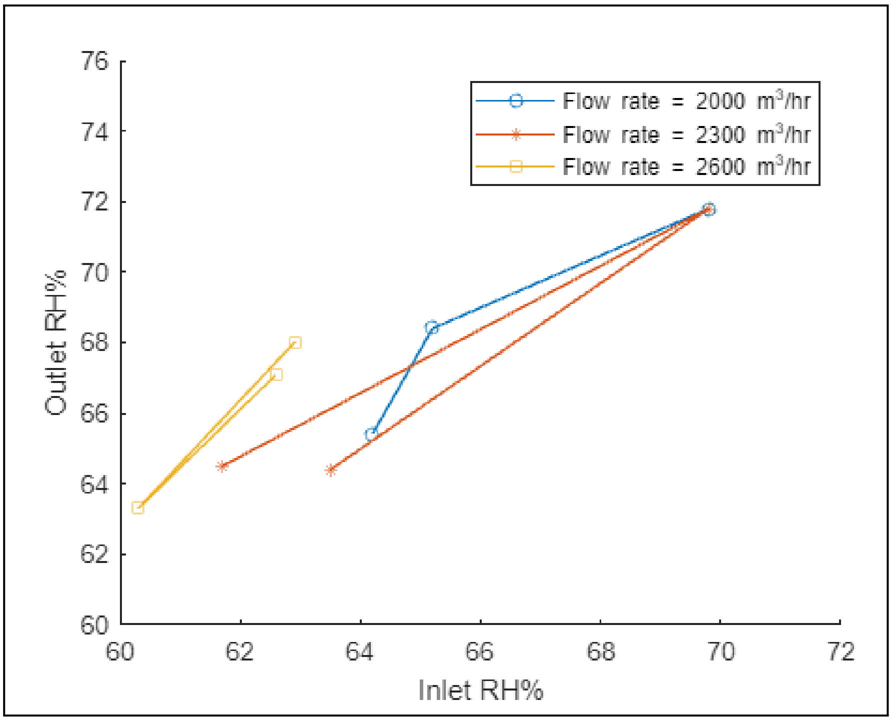

Fig. 8.2. Experiments on RH with varying supply flow rate

8.2. VARYING THE SUCTION BLOWER FLOW RATE

Flow rate (m^3/hr)	DBT (℃)			WBT (℃)		DP (℃)		RH (%)	
	Inlet	**Outlet**	**ΔDBT**	**Inlet**	**Outlet**	**Inlet**	**Outlet**	**Inlet**	**Outlet**
0	33.1	31.2	**1.9**	27.1	26.1	24.8	24.2	62.2	65.3
	32.5	32.0	**0.5**	26.4	26.2	24.0	23.9	61.2	62.5
	32.1	31.0	**1.1**	26.7	26.3	24.6	24.5	64.8	68.1
180	34.3	31.8	**2.5**	25.1	26.4	27.5	24.3	60.2	63.6
	32.8	32.0	**0.8**	26.5	25.7	24.1	23.3	60.4	63.1
	31.8	31.1	**0.7**	26.9	26.8	25.1	25.0	67.8	70.4
450	33.4	31.6	**1.8**	26.9	26.5	24.7	24.5	61.0	64.3
	33.1	32.0	**1.1**	26.1	25.5	23.2	23.0	56.2	59.1
	31.6	31.1	**0.5**	26.8	26.6	25.0	24.9	67.9	69.9

Table 8.2. Experiments by varying suction blower flow rate

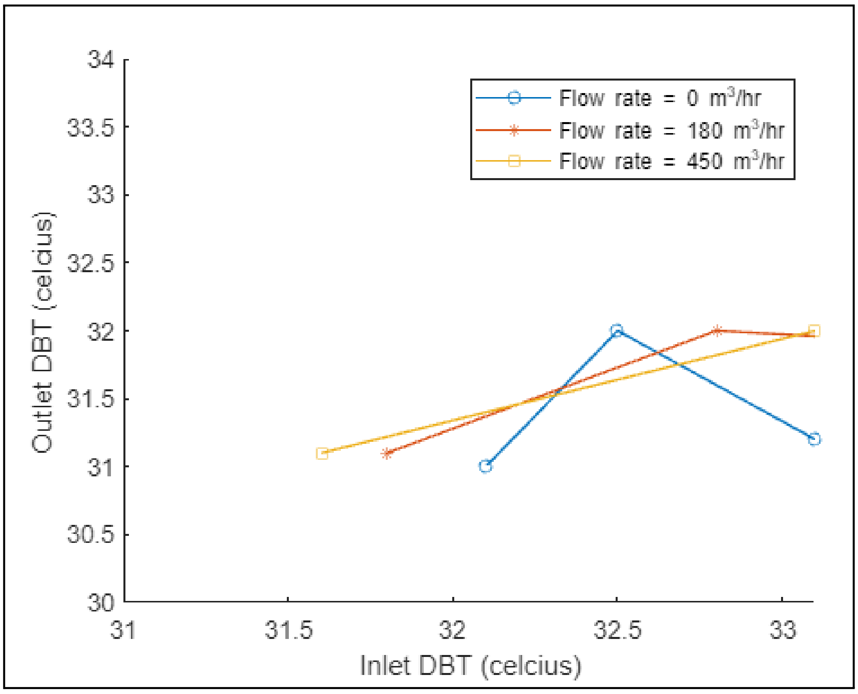

Fig. 8.3. Experiments on DBT with varying suction flow rate

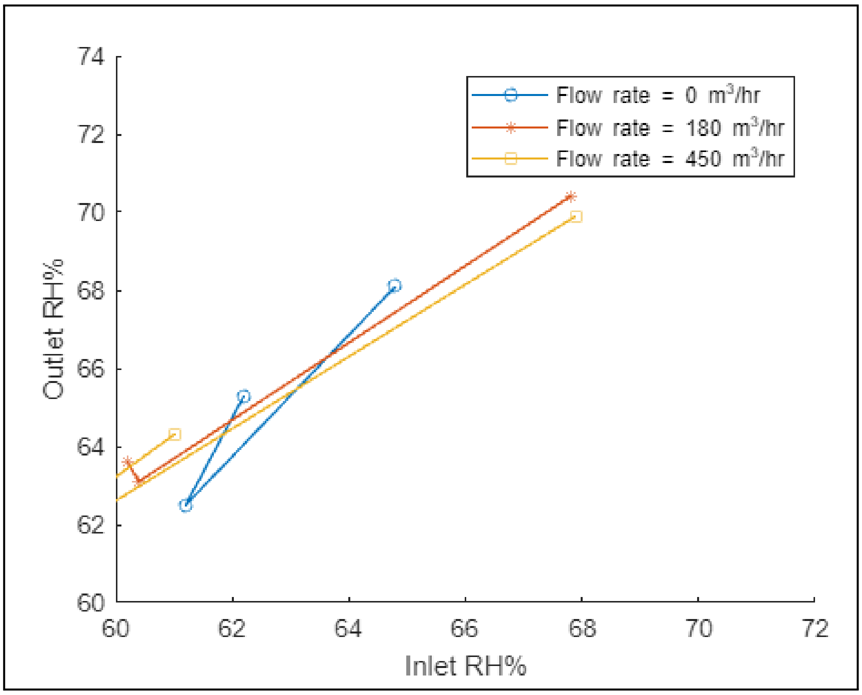

Fig. 8.4. Experiments on RH with varying suction flow rate

8.3. CONCLUSION

The experiment was conducted by observing the DBT, WBT, Dew Point (DP) and the Relative Humidity (RH) of the outlet air by varying the flow rates of the supply blower and the suction blowers respectively. It was observed that the greater ∆DBT of 2.4 ℃ and 2.5 ℃ is achieved at the flow rates of 2600 m^3/hr and 180 m^3/hr of the supply blower and the suction blower respectively. This shows that the flow rate of the blowers directly influences the temperature drop i.e. temperature drop is directly proportional to the flow rate of the blower.

The experimental results also show that the greater temperature drop is achieved with higher inlet temperature. This shows that the developed system is suitable for regions with hot and arid climatic conditions.

The change in the RH% of the inlet and the outlet of the system is relatively low in the range of 4%. Therefore, the supply air from the outlet with a temperature drop without added humidity is achieved.

8.4. SCOPE FOR FUTURE WORKS

- The numerical simulation is done only for the analysis of uniform flow distribution whereas the evaporation process in HMX which includes the mass transfer should be done.

- The suction blower controller with PWM of the blower is designed and circuit is developed but only the manual control of the blower is installed to the system. The PWM controller should be installed that will ease the control just by using the IR transmitter.

- The water level monitoring system is planned while designing the controller of the system. The float sensor with appropriate controlling parameters and programming code should be added.

- The overall dimension of the system planned was altered due to increase in size of the wet channels designed. The future product should focus on the compactness of the system.

REFERENCES

[1] S. Chakraborty, D. Vernon, A. Jha, V. Narayanan, Performance characterization of M-cycle indirect evaporative cooler and heat recovery ventilator for commercial buildings - Experiments and model, Energy & Buildings 281 (2023) 112762, https://doi.org/10.1016/j.enbuild.2022.112762

[2] C. Zhan, X. Zhao, S. Smith, S.B. Riffat, Numerical study of a M-cycle cross-flow heat exchanger for indirect evaporative cooling, Building and Environment 46 (3) (2011) 657-668, https://doi.org/10.1016/j.buildenv.2010.09.011

[3] H. S. Dizaji, E. Hu, L. Chen, S. Pourhedayat, M. Wae-hayee, Proposing the concept of mini Maisotsenko cycle cooler for electronic cooling purposes; experimental study, Case Studies in Thermal Engineering 27 (2021) 101325, https://doi.org/10.1016/j.csite.2021.101325

[4] A. K. Gupta, S. Kashyap, J. Sarkar, Machine learning model of regenerative evaporative cooler for performance prediction based on experimental investigation, International Journal of Refrigeration 137 (2022) 178-187, https://doi.org/10.1016/j.ijrefrig.2022.02.006

[5] U. Sajjad, N. Abbas, K. Hamid, S. Abbas, I. Hussain, S. M. Ammar, M. Sultan, H. M. Ali, M. Hussain, T. U. Rehman, C. C. Wang, A review of recent advances in indirect evaporative cooling technology, International Communications in Heat and Mass Transfer 122 (2021) 105140, https://doi.org/10.1016/j.icheatmasstransfer.2021.105140

[6] S. Kumar, S. S. Salins, S. V. K. Reddy, P. S. Nair, Comparative performance analysis of a static & dynamic evaporative cooling pads for varied climatic conditions, Energy 233 (2021) 121136, https://doi.org/10.1016/j.energy.2021.121136

[7] S. D. Kadam, M. Garg, H. J. Palanthandalam-Madapusi, Assessment of Passive Evaporative Cooling Measures on the IIT Gandhinagar Campus, IJERT 10 (10) (2021) 2278-0181, DOI : 10.17577/IJERTV10IS100172

[8] Q. Chen, M. K. Ja, M. Burhan, M. W. Shahzad, D. Ybyraiymkul, H. Zheng, K. C. Ng, Experimental study of a sustainable cooling process hybridizing indirect evaporative cooling and mechanical vapor compression, Energy Reports 8 (2022) 7945-7956, https://doi.org/10.1016/j.egyr.2022.06.019

[9] H. M. Asfahan, U. Sajjad, M. Sultan, I. Hussain, K. Hamid, M. Ali, C. C. Wang, R. R. Shamshiri, M. U. Khan, Artificial Intelligence for the Prediction of the Thermal Performance of Evaporative Cooling Systems, Energies 14 (13) 2021 3946, https://doi.org/10.3390/en14133946

[10] D. Pandelidis, A. Cichoń, A. Pacak, P. Drag, M. Drag, W. Worek, S. Cetin, Performance study of the cross-flow Maisotsenko cycle in humid climate conditions, International Communications in Heat and Mass Transfer 115 (2020) 104581, https://doi.org/10.1016/j.icheatmasstransfer.2020.104581

[11] J. Chu, X. Huang, Research status and development trends of evaporative cooling air-conditioning technology in data centers, Energy and Built Environment 4 (1) (2023) 86-110, https://doi.org/10.1016/j.enbenv.2021.08.004

[12] S. Kashyap, J. Sarkar, A. Kumar, Proposal and month-wise performance evaluation of a novel dual-mode evaporative cooler, Heat and Mass Transfer 55(2019) 3523–3536, https://doi.org/10.1007/s00231-019-02670-6

[13] R. Boukhanouf, O. Amer, H. Ibrahim, J. Calautit, Design and performance analysis of a regenerative evaporative cooler for cooling of buildings in arid climates, Building and Environment 142 (2018) 1-10, https://doi.org/10.1016/j.buildenv.2018.06.004

[14] A. K. Dhamneya, S. P. S. Rajput, A. Singh, Thermodynamic performance analysis of direct evaporative cooling system for increased heat and mass transfer area, Ain Shams Engineering Journal 9 (4) (2018) 2951-2960, https://doi.org/10.1016/j.asej.2017.09.008

[15] R. S. Bindu, N. Kumar, N. P. Choudhary, A. Naik, P. Gupta, Design of Indirect Evaporative Cooler Flat Plate-Counter Flow Type. IJERT 6 6 (2017) 2278-0181**,** http://dx.doi.org/10.17577/IJERTV6IS060118

[16] E. D. Rogdakis, D. N. Tertipis, Maisotsenko cycle: technology overview and energy-saving potential in cooling systems, Energy and Emission Control Technologies 3 (2015) 15–22, https://doi.org/10.2147/EECT.S62995

[17] T. Sun, X. Huang, Y. Chen, H. Zhang, Experimental investigation of water spraying in an indirect evaporative cooler from nozzle type and spray strategy perspectives, Energy and Buildings 214 (2020) 109871, https://doi.org/10.1016/j.enbuild.2020.109871

[18] L. Chen, J. Shen, Y. Ge, Z. Wu, W. Wang, F. Zhu, H. Feng, Power and efficiency optimization of open Maisotsenko-Brayton cycle and performance comparison with traditional open regenerative Brayton cycle, Energy Conversion and Management 217 (2020) 113001, https://doi.org/10.1016/j.enconman.2020.113001

[19] H. Jafarian, H. Sayyaadi, F. Torabi, Modeling and optimization of dew-point evaporative coolers based on a developed GMDH-type neural network, Energy Conversion and Management 143 (2017) 49-65, https://doi.org/10.1016/j.enconman.2017.03.015

[20] M. H. Mahmood, M. Sultan, T. Miyazaki, S. Koyama, V. S. Maisotsenko, Overview of the Maisotsenko cycle – A way towards dew point evaporative cooling, Renewable and sustainable energy reviews 66 (2016) 537-555, https://doi.org/10.1016/j.rser.2016.08.022

APPENDIX

APPENDIX A - programming code for supply blower controller

```
#include <IRremote.h>
#define RELAY1 2
#define RELAY2 3
#define RELAY3 4
#define RELAY4 5

// Create an instance of the IRremote library.
IRrecv irrecv(6);
decode_results results;

void setup()
{
// Set up the four relay pins as output.
  pinMode(RELAY1, OUTPUT);
  pinMode(RELAY2, OUTPUT);
  pinMode(RELAY3, OUTPUT);
  pinMode(RELAY4, OUTPUT);

// Set all relays off initially.
  digitalWrite(RELAY1, HIGH);
  digitalWrite(RELAY2, HIGH);
  digitalWrite(RELAY3, HIGH);
  digitalWrite(RELAY4, HIGH);

// Start the IR receiver.
  irrecv.enableIRIn();
// Start the serial communication with a baud rate of 9600.
  Serial.begin(9600);
}
```

```
void loop()
{
// If we've received an IR signal, decode it and take action.
  if (irrecv.decode(&results))
  {
    Serial.print("0x");
    Serial.println(results.value, HEX); // Print the hex value of
the IR code received.

    switch (results.value)
    {
      case 0xA90:
        digitalWrite(RELAY1, HIGH);
        digitalWrite(RELAY2, HIGH);
        digitalWrite(RELAY3, HIGH);
        digitalWrite(RELAY4, HIGH);
        break;
// Button 1 on remote turns on relay 1 and turns off other relays.
      case 0x10:
        digitalWrite(RELAY1, LOW);
        digitalWrite(RELAY2, HIGH);
        digitalWrite(RELAY3, HIGH);
        digitalWrite(RELAY4, HIGH);
        break;

// Button 2 on remote turns on relay 2 and turns off other relays.
      case 0x810:
        digitalWrite(RELAY2, LOW);
        digitalWrite(RELAY1, HIGH);
        digitalWrite(RELAY3, HIGH);
        digitalWrite(RELAY4, HIGH);
        break;
```

```
// Button 3 on remote turns on relay 3 and turns off other relays.
      case 0x410:
        digitalWrite(RELAY3, LOW);
        digitalWrite(RELAY1, HIGH);
        digitalWrite(RELAY2, HIGH);
        digitalWrite(RELAY4, HIGH);
        break;

// Button 4 on remote turns on relay 4 and turns off other relays.
      case 0xC10:
        digitalWrite(RELAY4, LOW);
        digitalWrite(RELAY1, HIGH);
        digitalWrite(RELAY2, HIGH);
        digitalWrite(RELAY3, HIGH);
        break;

// Ignore any other button presses.
      default:
        break;
    }

    switch (results.value)
    {
// Button 1 on remote turns on relay 1 and turns off other relays.
      case 0x2F0:
        digitalWrite(RELAY1, LOW);
        digitalWrite(RELAY2, HIGH);
        digitalWrite(RELAY3, HIGH);
        digitalWrite(RELAY4, HIGH);
        break;
```

```
// Button 2 on remote turns on relay 2 and turns off other relays.
      case 0xCD0:
        digitalWrite(RELAY2, LOW);
        digitalWrite(RELAY1, HIGH);
        digitalWrite(RELAY3, HIGH);
        digitalWrite(RELAY4, HIGH);
        break;

// Button 3 on remote turns on relay 3 and turns off other relays.
      case 0xAF0:
        digitalWrite(RELAY3, LOW);
        digitalWrite(RELAY1, HIGH);
        digitalWrite(RELAY2, HIGH);
        digitalWrite(RELAY4, HIGH);
        break;

// Button 4 on remote turns on relay 4 and turns off other relays.
      case 0x2D0:
        digitalWrite(RELAY4, LOW);
        digitalWrite(RELAY1, HIGH);
        digitalWrite(RELAY2, HIGH);
        digitalWrite(RELAY3, HIGH);
        break;

// Ignore any other button presses.
      default:
        break;
    }
// Clear the received IR signal and enable the receiver to receive
the next signal.
    irrecv.resume();
  }
}
```

APPENDIX B - programming code for suction blower controller

```
#include <LiquidCrystal.h>
LiquidCrystal lcd(2, 3, 4, 5, 6, 7);
#define potentiometer  A0  //10k Variable Resistor
#define bt_F A1 // Clockwise Button
#define bt_S A2 // Stop Button
#define bt_B A3 // Anticlockwise Button
#define M1_Ena 11 // Enable1 L298 for PWM
#define M1_in1 10 // In1  L298 for Clockwise
#define M1_in2 9  // In2  L298 for Anticlockwise

int read_ADC =0;
int duty_cycle;
int duty_cycle_lcd;
int set = 0;

void setup(){
Serial.begin(9600);// initialize serial communication at 9600 bits
per second:
pinMode(potentiometer, INPUT);
pinMode(bt_F, INPUT_PULLUP);
pinMode(bt_S, INPUT_PULLUP);
pinMode(bt_B, INPUT_PULLUP);
pinMode(M1_Ena, OUTPUT);
pinMode(M1_in1, OUTPUT);
pinMode(M1_in2, OUTPUT);

lcd.begin(16,2);
lcd.setCursor(0,0);
lcd.print(" WELCOME To  My ");
lcd.setCursor(0,1);
lcd.print("YouTube  Channel");
delay(2000); // Waiting for a while
lcd.clear();
}
```

```
void loop(){
read_ADC = analogRead(potentiometer);
duty_cycle = map(read_ADC, 0, 1023, 0, 255);
duty_cycle_lcd = map(read_ADC, 0, 1023, 0, 100);
analogWrite(M1_Ena, duty_cycle);

lcd.setCursor(0,0);
lcd.print("Duty Cycle: ");
lcd.print(duty_cycle_lcd);
lcd.print("%  ");

if(digitalRead (bt_F) == 0){set = 1;}
if(digitalRead (bt_S) == 0){set = 0;}
if(digitalRead (bt_B) == 0){set = 2;}

lcd.setCursor(0,1);

if(set==0){ lcd.print("      Stop      ");
digitalWrite(M1_in1, LOW);
digitalWrite(M1_in2, LOW);
}
if(set==1){ lcd.print("    Clockwise   ");
digitalWrite(M1_in1, HIGH);
digitalWrite(M1_in2, LOW);
}
if(set==2){ lcd.print(" Anticlockwise  ");
digitalWrite(M1_in1, LOW);
digitalWrite(M1_in2, HIGH);
}
delay(50);
}
```